



Empa

Materials Science and Technology

VILNIUS UNIVERSITY
FACULTY OF CHEMISTRY
DEPARTMENT OF POLYMER CHEMISTRY

Vakarė Merkytė

Graduate studies Chemistry - 2 course

**SHAPING OF POROUS ZIRCONIUM OXIDE GRADIENT
STRUCTURES BY UV CURABLE, LATEX BASED
BINDERS**

Master's thesis

Supervisors: Prof. Ričardas Makuška

Prof. Thomas Graule

Ing. Caroline Durif

Evaluation: 2016 06 13

Vilnius/Dübendorf, 2016

CONTENT

ABBREVIATIONS	4
INTRODUCTION	5
1. LITERATURE REVIEW	6
1.1. TAPE CASTING	6
1.2. SLURRY FORMULATION	7
1.2.1. Powder	8
1.2.2. Surfactant	9
1.2.3. Solvent	10
1.2.4. Binder	11
1.2.5. Pore formers	11
1.2.6. Photoinitiator	12
1.2.7. Other additives	13
1.3. UV CURING	13
1.4. DEBINDING AND SINTERING	14
1.5. PROPERTIES OF CERAMIC TAPES	14
1.6. AREAS OF APPLICATION OF CERAMIC TAPES	15
2. EXPERIMENTAL PROCEDURE	18
2.1. MATERIALS	18
2.2. PRODUCTION PROCESS	19
2.2.1. Stabilisation of zirconia	19
2.2.2. Slurry preparation	19
2.2.3. Shaping procedure	19
2.2.5. Burning stage	19
2.3. DATA ANALYSIS PROCEDURES	21
2.3.1. Potentiometric titration	21
2.3.2. Rheological characterization	21
2.3.3. FTIR	21
2.3.4. SEM	21
2.3.5. Archimedes' method	22
3. RESULTS AND DISCUSSION	23
3.1. CHARACTERISATION OF DISPERSION	23
3.1.1. Selection of appropriate amount of surfactant	23
3.1.2. Effect of solid load on viscosity values	25
3.2. CHARACTERISATION OF UV CURING SYSTEM	28
3.2.1. UV induced free radical photopolymerisation of latex binder	28
3.2.2. Selection of appropriate amount of photoinitiator and UV curing time	30
3.3. CHARACTERISATION OF THE SINTERED SAMPLES	33
3.3.1. Shrinkage	33
3.3.2. Microstructure of the tapes sintered at 1500 °C and 1300 °C	34
3.3.3. Microstructure of the tapes sintered at 1150 °C	37
3.3.4. Density and porosity	38

CONCLUSIONS	40
SANTRAUKA	41
REFERENCES	42

Abbreviations

Bp	– boiling point
d₅₀	– median diameter
d₄²⁰	– density
DHC	– di-ammonium hydrogen citrate
FTIR	– Fourier transform infrared spectroscopy
I	– photoinitiator
IEP	– isoelectric point
M	– molecular mass
MIP	– mercury intrusion porosimetry
MLCC	– multilayered ceramic capacitors
MLCP	– multilayered ceramic packages
n_D²⁰	– refractive index
PF	– pore formers
SEM	– scanning electron microscopy
SOFC	– solid oxide fuel cell
SSA	– specific surface area
UV	– ultraviolet irradiation
YSZ	– yttria stabilised zirconia

Introduction

Tape casting is one of the most common production techniques of tapes in ceramics, metals and glass processing. This low cost method allows an adequate thickness control, to obtain high quality surfaces and multilayered structures. Tape casting was invented in 1946 by Glenn N. Howatt, who was working in the Massachusetts Institute of Technology. At first, it was used for the elaboration of ceramic capacitors. Since then, this technology has evolved and is routinely used today in many industries. Tape casting could be called doctor blading or knife coating as well [1-3].

Ceramic films are produced from the dispersion, which is named slurry. It contains ceramic components, solvents and organic additives. They are important for the rheology of the slurry. Moreover, organic additives guarantee the cohesion and flexibility of the films after drying or curing processes and are eliminated in the composite burning stage, known as debinding and sintering. In this work, the submicron zirconium oxide is used as the ceramic powder due to its superior chemical, physical and thermal stability, ionic conductivity, large specific surface area and good hydrophilicity. Latex based binders act as solvent and makes the slurry water-based system. Aqueous tape casting technique is gaining more and more attention, as an eco-friendly and cheap alternative [2, 4, 5].

Tape casting is broaden the scope of the use of ceramic materials in engineering and electronic industries. Porous ceramics have a wide variety of promising commercial applications in filters, gas burners, fuel-cell electrodes, battery separators, membrane reactors and many more. Most of these applications have rather strict requirements in terms of the morphology. A gradient structure in the porosity of tapes is an advantage and could be successfully adjusted for the manufacture of solid electrolytes for the sensors and solid fuel cells [1, 6-8].

The aim of this work is to shape and characterise good quality porous zirconium oxide gradient structures produced with UV curable, latex based binders.

Tasks of this work:

1. To prepare stable and homogeneous slurry and investigate its properties with zeta potential and rheological measurements.
2. To produce UV curable and water-based green tapes with porous structure.
3. To characterise tapes after debinding and sintering with SEM technique.

1. LITERATURE REVIEW

1.1. Tape casting

Tape casting is a well-established technique used for large-scale fabrication of ceramic, metal, glass substrates and multilayered structures. This method lets to achieve high quality two dimensional structures, large in the x and y direction and very thin in the z dimension, which is highly required for ceramics used for electronical applications. There are some differences between tape casting and other traditional ceramic forming processes to produce thin layers, such as dry pressing, slip casting, extrusion plus calendering, dry powder roll compaction, screen printing and electrophoretic deposition. Tape casting offers the widest thickness range (approx. 10 – 1000 μm) and the thinnest self-supporting layers. It has no fundamental restrictions concerning the use of the binder and/or solvent systems. Moreover, it gives a smooth surface to flexible ceramic tapes. Although, disadvantages of this technique could appear at the drying or debinding and sintering stage [6, 9].

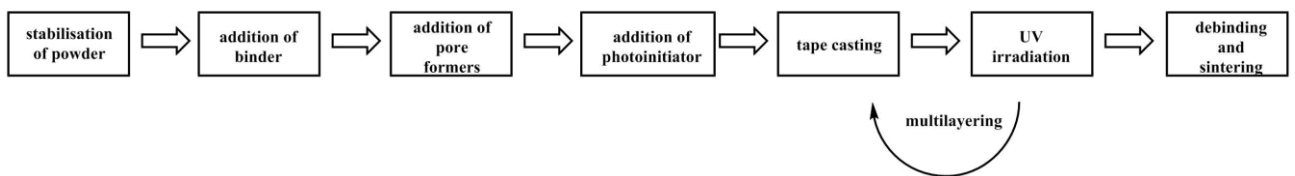


Fig. 1. Illustration of the tape production process

Classical tape casting process consists of three main stages – preparation of a stable ceramic dispersion in the water or organic solvent with organic additives, casting it onto a surface and burning out solvents and other additives. Fig. 1 shows the typical tape production process in smaller subsections. The first step is to stabilise ceramic powder. The coated powder is placed in a vessel and then organic materials and solvents are added. After each addition, the dispersion must be homogenised by milling or ultrasonication for some amount of time. The final dispersion is called slurry. In the second step, the slurry is placed in a container behind the doctor blade (see in Fig. 2) and casted onto the stationary or moving surface. If a photoinitiator is used, produced green tapes are placed in the UV box and cured. If the slurry do not contains the photoinitiator, green tapes are dried at the room temperature until the solvent is evaporated. When the UV-curing/drying stage is done, another layer of the tape could be casted on the first one and a multilayered structure could be achieved. To have the final product, the green tape is cut to an appropriate shape, debinded, and sintered in the oven. This is the last stage [6, 10].

Fig. 2 illustrates the principle of the tape casting with the stationary substrate and moving doctor blade. The green arrow shows the casting direction. In the tape caster, there is a glass plate

on which a substrate is stuck. Substrates differ in the material, coating and roughness. A strong dewetting behaviour and a not-removable phenomenon were always occurred problems. To solve these complications the different kind of substrate must be adjusted for each slurry with different powders, organic additives and solvents. In this thesis, it is a polyester film (Hostophan® RN 75 2 SLK sheet). Although the substrate could be any smooth surface, such as a glass or a polymer. Also, they are depending on the function of the equipment. Green tapes are shaped using a double doctor blade with a specified gap, which induces a thickness of the green tape. The double doctor blade controls hydrodynamic forces behind the casting blade better than casting with a single doctor blade. The gap is not fixed and can be adjusted using micrometers. When the slurry is poured into the doctor blade container, it must be kept there for 30 – 60 seconds before the start of the casting process in order to let rheological stresses, accumulated while slurry pouring to relax. The thickness of the resulting ceramic sheet can be reduced to less than a half of that, after the sheet is dried or burned out and this change must be considered when planning the fabrication [1, 6, 10, 11].

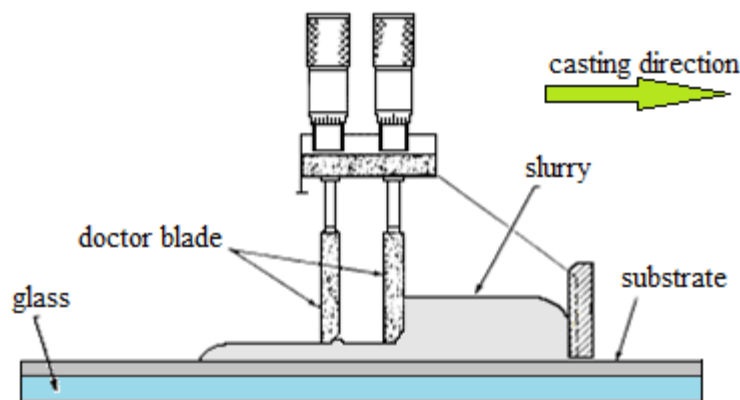


Fig. 2. Illustration of the tape casting principle

In the following sections, other stages of the tape production process are described. As well as, various types of materials which could be used for making the slurry.

1.2. Slurry formulation

Slurry preparation is the most important part of the experimental procedure. All results are based on this step and have an impact on the manufacturing method. Some general rules can be inferred for the preparation of the tape casting slurry. Firstly, the ratio between organic additives and ceramic powder must be as low as possible. Secondly, the amount of solvent must be fixed at the minimum to maintain a homogeneous slurry, which results in less curing and sintering shrinkage. Besides, the amount of surfactant must be the minimum necessary to ensure the stability of the slurry. And lastly, the photoinitiator to binder ratio must be adjusted to make the tape flexible, resistant and easy to release. Organic additives affect the slurry behaviour as well as

properties of the tape casted substrates. The composition of the slurry should be optimized in order to obtain green tapes, crack-free with high and an uniformly green density, which will densify to a high density after debinding and sintering stage [12].

1.2.1. Powder

Powder is the most important ingredient in the slurry formulation. After organic additives removal, the powder is the only portion of the slurry left and it determines properties of produced tapes. It is not possible to define a special set of powder characteristics suitable for tape casting. The choice has to be made according to demands of the present application and with the respect to criteria such as: chemical purity, particle size and size distribution, particle morphology, degree of aggregation or agglomeration, compositional homogeneity, sintering activity, ability to be mass-produce and costs of production. Ceramic powders either consist of single oxide (Al_2O_3 , BeO , MgO) or non-oxide components (AlN , SiC , ZrB_2), a prereacted complex combination with a well-defined chemical formula (BaTiO_3 , SrLaMnO_3), or a mixture of two or more of these substances ($\text{Al}_2\text{O}_3 + \text{ZrO}_2$, $\text{ZrB}_2 + \text{SiC}$) [2, 9, 10, 13-16].

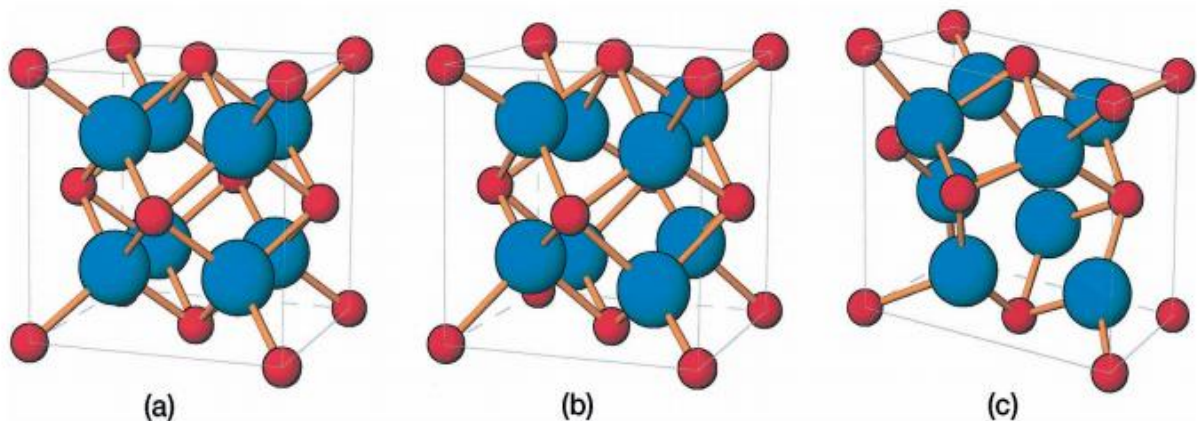


Fig. 3. Schematic representation of three polymorphs of the ZrO_2 : (a) cubic, (b) tetragonal and (c) monoclinic [17]

Zirconium, as a basic element, is shiny silver metal, which is relatively soft, flexible and heavy. It is ranked as the 17th of the most common elements on the Earth. The oxide of this metal is called zirconia. Zirconium oxide is a very important industrial ceramic, due to its high toughness, which has proven to be superior to other ceramics. Also, it has high chemical, physical and thermal stability, high ionic conductivity, low coefficient of friction and wear resistance. These properties are strongly required in electronics. Furthermore, zirconia shows excellent biocompatibility and bioinertness coupled with good mechanical properties, that makes it suitable as the biomaterial [18, 19].

The thermodynamically stable, room temperature form of zirconia is baddeleyite. But this mineral is not widely used for industrial applications. Fig. 3 shows three low pressure phases of the zirconia: monoclinic, tetragonal and cubic, which are stable at increasingly higher temperature. The monoclinic phase is stable up to 1170 °C, while the tetragonal phase is stable between 1170 and 2370 °C, and the cubic one – above 2370 °C. The higher stability is the monoclinic phase. That can confirm the results of calculated energy versus volume data at zero absolute temperature. However, most engineering applications are by using cubic and tetragonal phases. During the cooling process, the phase transformation from tetragonal to monoclinic is a reversible athermal martensitic transformation, which is associated with a finite amount of volume change (approx. 4 %). This leads to disintegration of the undoped polycrystallised zirconia ceramics. The inducing high stress results cracks in the ceramic structure. This disruptive phase change is eliminated by stabilising the cubic form of zirconia with solid solutions of CaO, Y₂O₃, Yb₂O₃, Nd₂O₃ or Sc₂O₃. Fig. 4 shows the principal of the insertion of the Y₂O₃ inside the ZrO₂ lattice. Stabilisation is carried out at the room temperature with significant amounts (above 8 mol%) of dopants. With less amount of dopant (below 8 mol%) the tetragonal could be stabilised. The electrical resistivity of yttria- and calcia-stabilised zirconia decreases with temperature, primarily owing to the increase in the oxygen on the diffusion rate. This property has led to use stabilised zirconia for the electrolyte in high-temperated fuel cells [17-20].

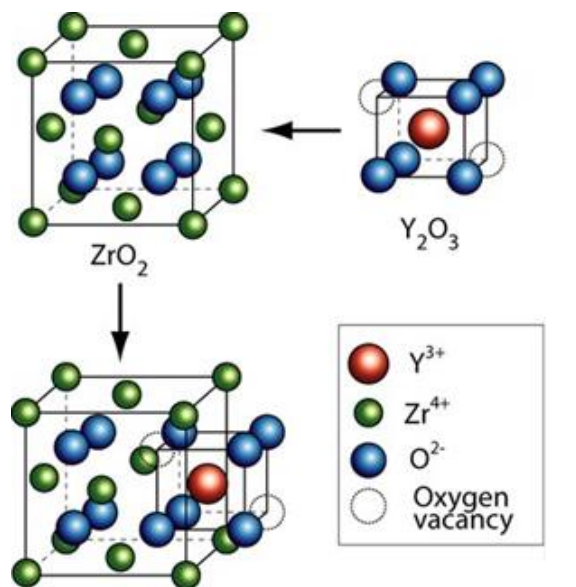


Fig. 4. Illustration of the insertion of the yttrium oxide inside the zirconia oxide lattice [21]

1.2.2. Surfactant

Small powder particles have a pronounced tendency to arrange themselves in large agglomerates, so due to this reason, the ceramic powder dispersions in liquids are usually very unstable and inhomogeneous. The uncontrolled agglomeration in the slurry would have undesirable

consequences for the further processing and properties of the green tape. Agglomerates can be explained with the interaction of particles. In the area of the isoelectric point (IEP), attractive Van der Waals forces are not compensated by electrostatic forces which result in attracted particle accumulations. To achieve an adequate distance between particles, the surface charge needs to be changed or by coating particles with an organic barrier layer. The combination of these two methods could be done with polyelectrolytes (e.g. poly(methacrylic acid), sodium polyphosphates). Surfactants cause the change of the surface charge by adsorption on the particle surface. There are various surfactants, for instance, sodium oxalate, pyrophosphates – which contain potential determining anions. When adsorbed on the oxide powder surface, they decrease the pH of the IEP with a consequent increase in the negative zeta potential at the given pH. Di-ammonium hydrogen citrate (DHC) is a well known dispersant used for preparation of aqueous ceramic powder dispersions, which show lower viscosity at higher solids loading [10, 21-25].

1.2.3. Solvent

The main tasks of solvents are: dissolving organic additives, dispersing ceramic powder particles, providing suitable viscosity and guaranteeing flawless consolidation of tapes. Traditionally organic solvents have been used, such as butyl acetate, methyl ethyl ketone, trichloroethylene or various azeotropic binary mixtures (e.g. ethanol/butanol, ethanol/methyl ethyl ketone, isopropanol/toluene). Organic solvents have a low viscosity, a low boiling point and a high vapour pressure. However, they are also flammable and toxic [9-11, 14, 26].

Today, water based tape casting is more commonly used by the industry and within the research area. There are lots of scientific articles which could prove that aqueous dispersions are suitable for the tape casting and let to achieve ceramics with very high final sintered densities. An aqueous media enables high purity, smooth substrates produced without using environmentally damaging solvents. Water has advantages of being non-toxic, non-flammable, easily available and cheap. Although, in comparison with organic solvent based slurries, aqueous tape casting systems have a smaller tolerance to minor changes in processing parameters [5-7, 12, 13, 15].

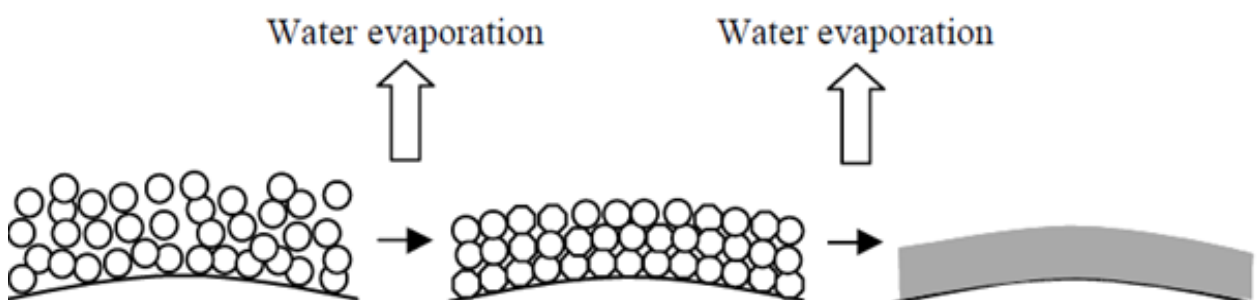


Fig. 5. Mechanism of drying using an aqueous media

There are two ways to remove the solvent from the green tape: dry it at the room temperature or add a photoinitiator in the slurry composition and to cure the casted tape with the UV light. Fig. 5 shows the mechanism of the water evaporation. At first, an aqueous dispersion is deposited on the tablet surface. In the second stage, polymer particles compact and deform. Finally, coalescence into a continuous film is observed. The curing mechanism, advantages and problems of those two mechanisms are described in a section 1.3.

1.2.4. Binder

Binder is the most important organic additive of the slurry. It supplies the network that holds the entire chemical system together for the additional processing. Furthermore, the binder has a huge effect on such green tape properties as strength, flexibility, plasticity, laminatability, durability, toughness, printability and smoothness. By adding the binder, a viscosity and an elastic modulus of the ceramic dispersion are increasing [9, 10].

Two groups of binders are mainly used for the casting of ceramics: cellulose ethers and vinyl or acrylic type monomers. In the organic media nitrocellulose, poly(vinyl chloride), poly(methyl methacrylate) could be dissolved and for the aquacasting ethyl cellulose, poly(vinyl alcohol) or acrylics based latex are used. Comparing to other polymers, acrylates are cheap, have a cleaner removal in neutral or reducing atmospheres, distinguish in strength and solubility and present a good reactivity towards UV radiations. Besides, they have different decomposition mechanisms. While vinyl binders oxidises, acrylic polymers disassemble and evaporate. So, these kind of binders are perfect for powders, which require reducing or inert atmospheres, such as high purity SiC, AlN or metal powders [6, 9, 10, 27].

1.2.5. Pore formers

Porous ceramics with open pore structures have an excellent permeability and a large surface area. For this purpose pore formers (PF) are added to the slurry to obtain porous ceramic sheets. In the debinding stage, PF will be burn out and leave the porous structure. After firing, concentration, composition and shape of PF particles have an influence of the final tape. The high temperature treatment also has an impact on the total porosity and changes the micro-porosity of the products [28-31].

During tape casting non-spherical particles, such as binder and PF are oriented in the tape casting direction due to of the shearing forces that occur when slurry passes below the doctor blade. It is known that bigger particles have the tendency to orient more than smaller particles due to the increased rotation velocity when perpendicular to the tape casting direction. If PF particles orient parallel to the casting direction, they will contribute to a higher pressure drop comparing with PF

particles, which orient perpendicular. Hence the desirable pore orientation is perpendicular to the tape casting direction [31].

Numerous PF are known, including starch, graphite, sucrose, polystyrene, polypropylene, poly(methyl methacrylate) and etc. Starch is the most frequently used, due to its biological origin and availability, but the difficulties in maintaining the pore structure burn out and the narrow size range of commercially available starch types (between 5 – 50 μm) limits its application when large pores are desirable. A good alternative is represented by polymers. They exhibit burn out stage without defects at relatively low temperatures and are easily mixed with ceramic powder. Furthermore, polymeric PF are very cheap and relatively sustainable [7, 29, 30].

1.2.6. Photoinitiator

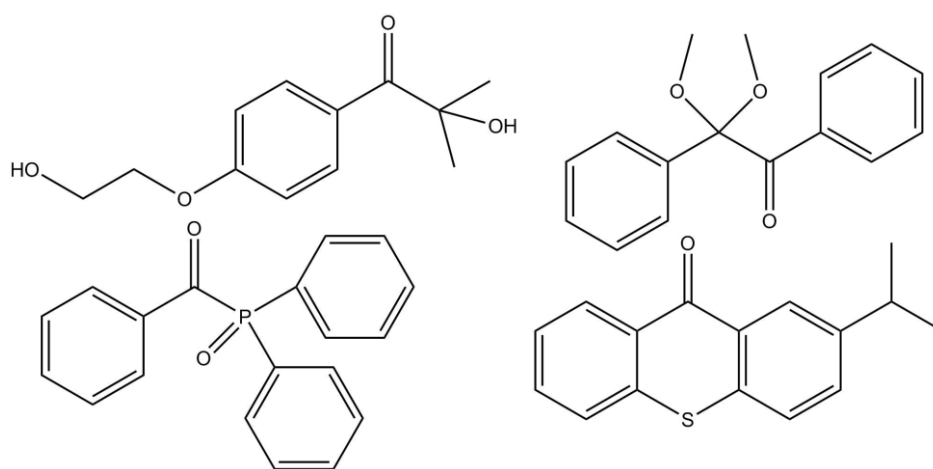


Fig. 6. Different types of photoinitiators

Photoinitiator starts a radical polymerization reaction when exposed to UV light and enables to reach high conversions of the monomer in a short irradiation time. The most important class of photoinitiators are aromatic carbonyl compounds with absorption in the UV and near visible ranges. These compounds are responsible for the efficient transformation of the energy of light into chemical energy in form of reactive species, that are capable of initiating the curing reaction. There are two ways to produce radicals using photoinitiators – to initiate the photopolymerisation reaction by bond cleavage (type I) or H-abstraction type (type II). In the Fig. 6 some photoinitiators are shown. Type I initiators undergo a homolytic alpha-cleavage of a carbonyl or carbonylphosphinoyl bond when irradiated with light. Polymerisation with type I initiators presents faster kinetics under short irradiation times with improved functional group conversion, reduced monomer elution and improved mechanical properties. Type II photoinitiators require the presence of a coinitiator (usually an amine) in the solution to work and give a bit slower initiating process [32, 33].

1.2.7. Other additives

Some functional additives could be used such as wetting agents, defoamers, homogenisers, preservatives, flow control agents and flocculants. They provide special slurry properties or led to establish desired characteristics in the cured tape. Wetting agents can be non-ionic (e.g. glycerol esters), anionic (e.g. sulfosuccinates), cationic (e.g. amines from fatty acids) or zwitterionic (e.g. methylamine salts of polycarbonic acids). These surface active agents are primarily soluble in the liquid phase, which are required to reduce the surface tension of the liquids and enhance their wetting properties for powders and substrates. Defoamers (e.g. fatty alcohols, poly(ethylene glycol)) are mostly used in the aqueous media to take off harmful stable foams from polymer solutions or dispersions, which are likely to occur during milling stage. It is much more effective to prevent foam formation than to attempt to destroy the foams. Sometimes the slurry is being de-gassed under vacuum before tape casting to avoid air bubbles. Homogenisers (e.g. cyclohexanone) increase the mutual solubility of the components, the density and tensile strength of the tapes. Preservatives are added to suppress bacterial or fungal attacks. The main role of the flow control agents (e.g. liquid polyethylene) is to prevent the surface of the tape from drying too rapidly, which might provoke cracks. Flocculants are preventing the slurry from forming extremely high density sediments. They are counteractive to dispersing agents by shifting the pH of the dispersion to values close to IEP [6, 9, 34-38].

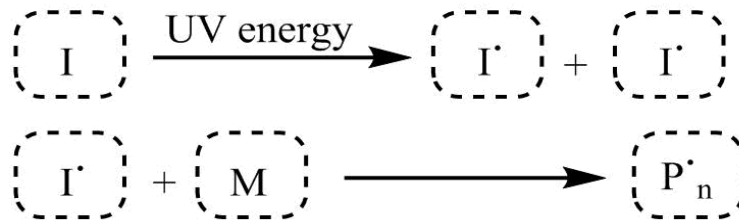
1.3. UV curing

The use of the photopolymerisable binder offers the advantage of eliminating the drying stage, which is a critical step of the tape casting process. If the tape is drying too fast, this may result in formation of a skin at the surface of the tape which reduces the evaporation rate and entraps gas bubbles. Also, it could occur formation of cracks within the tape and variation of the microstructure along the thickness of the tape due to the migration of the solvents. The shrinkage associated with drying is anisotropic and usually operates perpendicular to the sheet surface, thus generating residual stresses in the green tape. UV curing offers the possibility to lithographically pattern the slurry, obtain tapes without stresses, due to the low overall shrinkage. Furthermore, with UV curing the multilayered shape process is faster and the interface between two cured layers is a high quality [39, 40].

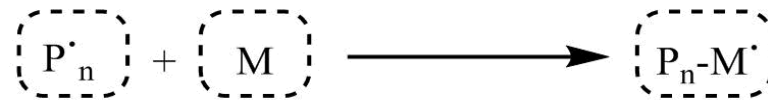
UV induced free radical photopolymerisation consists of three main stages, which are shown in the Fig. 7: initiation, propagation and termination. The initiation happens when the photoinitiator (I) is irradiated with the UV energy. The UV light is considered to be in the spectral range between 200 – 400 nm. A covalent bond in the molecules of initiator breaks and creates free radicals (I^\bullet). They react with a double bonded monomer (M) by forming growing polymer chain (P^\bullet_n). In the

propagation (II) the physical chain of the polymer is formed (P_n-M^\bullet). During this step, the molecular weight and crosslinking of the polymer are built. The propagation continues till no monomers are left or when the termination (III) occurs. The last photopolymerisation stage could end in two ways. The polymer chain (P_n-M^\bullet) reacts with another growing polymer chain (P_m^\bullet) or free radicals (I^\bullet). This stage produces the complete polymer chain.

(I) Initiation



(II) Propagation



(III) Termination

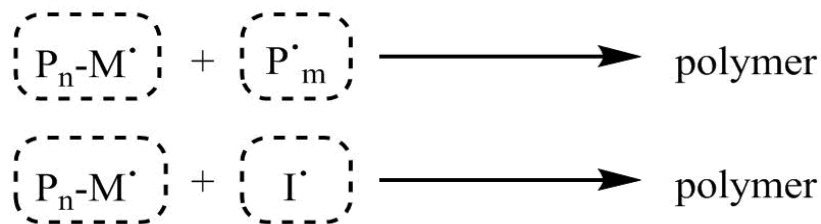


Fig. 7. Mechanism of the UV induced free radical photopolymerisation

1.4. Debinding and sintering

Green tapes contain large amounts of binder. Removing it before the sintering is considered as time consuming and delicate operation. The thermal removal of the binder remains as the most widely used and up to now irreplaceable method. During debinding process, green tapes are slowly heated until the binder decomposes and leaves the tape in the gaseous form. Usually this stage is based on three mechanisms: evaporation, thermal degradation and oxidative degradation. If binder consists of low molecular weight components, the evaporation can be faced. Binder components of the higher molecular weight are thermally degraded. The thermal degradation proceeds over the whole volume of the polymer phase. It also diffuses towards the tape surface or towards the liquid-vapour interface, where they evaporate. The presence of oxygen in the atmosphere during thermal extraction entails in the addition to the thermal degradation, also the oxidative degradation of the

polymer binder, which proceeds from the surface to the centre of the body and is limited by the diffusion of oxygen into the binder or by the diffusion of the products of degradation back to the surface and their evaporation. If the ceramic body is surrounded with an appropriate porous media, then the capillary forces make the binder flow from the body and extracted into the surrounding medium [9, 40, 41].

During debinding stage, all binders must be removed. Sintering temperatures are much more higher than the volatilization temperatures of the binders. This means, that any residual binder escaping rapidly from the tape could cause cracks and the tape lose its integrity or form some soot which may affect the properties of the material. Debinding and sintering stages could be executed separately or together. This depends on the materials which are being used for the manufacture of ceramic products [41-43].

The sintering induces a mechanical strength to ceramics by converting them into a strong part without losing the shape. The high temperature treatment not only influences the total porosity but it also changes the micro-porosity of the products. The sintering process is achieved by heating the consolidated mass of particles to the temperature, which is in the range between 50 – 80 % of the melting temperature. There are many different theories on the mechanism of sintering. The density after sintering is geometrically calculated out of the volume and mass of the sintered samples [41, 42].

1.5. Properties of ceramic tapes

In this thesis, a combination of water based and UV curable systems is examined. In the most studies, tapes are left for drying, instead of curing in the UV box at the particular wavelength. Although, the UV curing process minimises disadvantages caused by aqueous media in the tape casting technique. This chapter presents a short review of the properties of sintered tapes with a thickness approximately 100 – 200 μm , which were produced from the water based slurries or had those two methods combined.

The solid load in the zirconia ceramics has a wide breach due to different grain size powders, 40 – 80 wt %. Using distinct pore formers, the porosity varies from 14 to 45 % and the bending strength is between 230 – 750 \pm 100 MPa. The shrinkage after debinding and sintering can be 10 – 30 %, depending of the tape casting thickness, solvent system and an addition of UV curing stage. Less shrinkage is observed while having thinner tapes, aqueous media and UV curing instead of drying green tapes in the air. Another oxide ceramic powder which is usually combined with the aqueous media and photopolymerisation stage is alumina. The solid load is quite similar to zirconia slurries. Desired porosity is often the same as well. Although, some articles are presenting alumina tapes with porosity of 60 – 65 %. The bending strength of those tape is from 345 to 490 \pm 20 MPa

and thermal conductivity is from 1.3 to 6.5 W/m*K. While the thermal conductivity of zirconia tapes is around 0.9 W/m*K [5-7, 39, 40, 44-46].

Generally, non-oxide ceramics are fabricated by dry pressing or injection molding. However, the first technique has a high pressure which may cause delamination, and the other method has limitations of porosity. Manufacturing sheets by tape casting, with a powder consisting of non-oxide components, a drying stage is never replaced by UV curing. Also, literature studies on aqueous tape casting of these ceramics are relatively few, due to the slurry properties, which are more sensitive to the casting parameters. In the comparison of the oxide powders, the solid load of the slurry in the aluminium nitride ceramics is 70 – 80 wt %. Using aqueous media, the porosity of the sintered tapes is from 2.1 to 7.6 %, thermal conductivity – from 96 to 116 W/m*K and bending strength varies from 206 to 283 ± 20 MPa. When AlN tapes are prepared with organic media by using an azeotropic binary mixture, the solid load usually is lower – between 60 – 70 wt %. Slight changes in the properties of those ceramic sheets are observed and tapes are without open pores [47, 48].

1.6. Areas of application of ceramic tapes

Thin and flat ceramic substrates with multilayer structure mainly are used for electronic industry. The typical applications for multilayered tape cast products are solid electrolytes for sensors (e.g. an electrochemical reactor for flue gas purification) and solid fuel cells (SOFCs) [6, 7, 9, 28, 33, 49].

Solid electrolyte contains chemical compounds exhibiting practically only the ionic conductivity. Electrolyte passes an ionic current flowing inside an electrochemical cell that equals an electronic current flowing in an external circuit between electrodes on opposite side of the electrolyte. The driving force for the current flow is a chemical reaction between reactants on opposite sides of the electrolyte: a reductant at the negative electrode (the anode) and an oxidant at the positive electrode (the cathode). The use of a solid electrolyte simplifies the cell design, as well as improves safety and durability, comparing to the cells with liquid electrolyte. Ceramic materials are more suitable for rigid battery designs, because of high elastic moduli and an ability to use them in high temperature or other aggressive environments [49, 50].

SOFCs are the most efficient devices for the electrochemical conversion of chemical energy of hydrocarbon fuels into electricity. SOFC contains a solid oxide electrolyte, which is made from a ceramic. This ceramic acts as a conductor of oxide ions, allowing oxygen atoms to be reduced on its porous cathode surface by electrons. When oxygen atoms are converted into oxide ions, they are transported through the ceramic body to a fuel-rich porous anode zone where the oxide ions can react. Working temperature of SOFC is between 600 – 1000 °C. Zirconium oxide is generally used

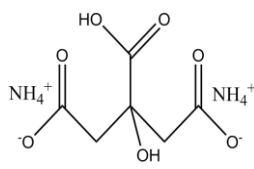
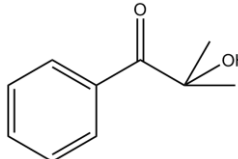

as the electrolyte due to its uniquely detection of the oxygen, superior stability and a low cost. Moreover, comparing to the other ceremics, zirconia exhibit a minimum electronic contribution to total conductivity in the oxygen partial pressure range. This ability is the most important for the practice ceramics application as fuel cells [8, 51, 52].

Products of tape casting can work as multilayered ceramic packages (MLCPs) or multilayered ceramic capacitors (MLCCs). MLCP is semiconductor device in a strong, thermally stable and hermetic environment. For making MLCPs, different kinds of Al_2O_3 is mostly used. In MLCC ceramic material acts as a dielectric and it can be paroelectric (e.g. TiO_2 , modified by Zr) or ferroelectric (e.g. BaTiO_3). Another application of ceramic tapes is a separator for batteries. It keeps the electrodes from touching and shorting out of the battery. Usually, separators are made of AlN , MgO or BN . Since size, structure and shape have significant influence on properties of the ceramics, structure-controlled materials could be manufactured by tape casting using various types of inorganic powders, as well [7, 10, 14].

Most of these applications have rather strict requirements in terms of the morphology. This could be easily achieved by tape casting method. Besides electronic industry, porous ceramics are used in a broad range of engineering applications. Such as filters for molten metals or particles in gas streams, in catalysis and separation, as load-bearing lightweight structures or for thermal and acoustic insulation [38].

2. EXPERIMENTAL PROCEDURE

2.1. Materials

Name of the material	Properties	Formula/composition
Di-ammonium hydrogen citrate, <i>Fluka</i>	M 226.19 d_4^{20} 1.48 g/cm ³	 C ₆ H ₁₄ N ₂ O ₇
Irgacure [®] 1173 (2-hydroxy-2-methyl-1-phenyl-1-propanone), <i>BASF</i>	M 164.20 d_4^{20} 1.08 g/cm ³ Bp 252 °C	 C ₁₀ H ₁₂ O ₂
1 M Hydrochloric acid solution, <i>Fluka</i>	M 36.46	HCl
Laromer [®] UA 9064, <i>BASF</i>	d_4^{20} 1.065 g/cm ³ Bp 100 °C pH 6.5-7.5	Urethane acrylate dispersion with 62 % water content
1-octanol, <i>Sigma-Aldrich</i>	M 130.23 d_4^{20} 0.847 g/cm ³ n_D^{20} 1.429 Bp 196 °C	 C ₈ H ₁₈ O
Pore former DPP 3710, <i>Trinseo</i>	d_{50} 140 nm pH 4.0-7.0	Dispersion of polystyrene 45-55 %, water 45-55 %, sodium dodecylbenzenesulfonate ≤ 1.5 %.
Pore former DPP 3720, <i>Trinseo</i>	d_{50} 260 nm pH 5.0-8.0	Dispersion of polystyrene 45-55 %, water 45-55 %.
Pore former DPP 3740, <i>Trinseo</i>	d_{50} 450 nm pH 4.0-7.0	Dispersion of polystyrene 50-60 %, water 40-50 %.
1 M Sodium hydroxide solution, <i>Fluka</i>	M 40.00	NaOH
Zirconium oxide (stabilised with 13% of yttrium oxide), <i>Tosoh</i>	d_4^{20} 5.98 g/cm ³ d_{50} 52 nm SSA 16.0 m ² /g	ZrO ₂ /Y ₂ O ₃

2.2. Production process

2.2.1. Stabilisation of zirconia

100 g of YSZ and 0.25 g of DHC (0.25 wt % of YSZ) were put in the container with 5 mm zirconium oxide milling balls and dispersed with deionized water (approximately 40 ml). The container was left for mixing on the roller bench for 24 h with speed of 50 rpm. Later, the dispersion was poured into the beaker and dried at 100 °C for 8 h. Dried powder was grinded with a mortar and a pestle. White, stabilised zirconia powder was kept in the sealed vessel at the room temperature.

2.2.2. Slurry preparation

100 g of the stabilised zirconia powder and 45 g of latex binders (45 wt % of zirconia) were put inside planetary mill jar with 5 mm zirconium oxide milling balls. The jar was placed in the planetary ball mill machine and mixed in the circular motions for 10 min at 200 rpm. After that, 10 g of pore formers (10 wt % of zirconia) were added and homogenised for 2 min at 200 rpm. Finally, 1.1 g of photoinitiator (2.5 wt % of latex binders) was dripped in the mixture and milled for 2 more minutes at the same speed. The white homogeneous slurry was poured into the sealed, impervious vessel and used for the tape casting on the same day as it was prepared.

2.2.3. Shaping procedure

Prepared slurry was added into doctor blade tank and kept approximately 30 s before the start of tape casting. The blade gap was fixed at a high of 150 µm with a constant speed of 30 cm/min. The slurry was casted onto 75 µm thick Hostophan® RN 75 2 SLK sheets (Mitsubishi GmbH) – polyester films. Then, 30 cm long tape was cut and taken to the UV box (Vilber Lourmat). It was cured for 30 min using a wavelength of 256 nm with five tubes of 8 W each. At last, FTIR analysis was done of those green tapes.

2.2.5. Burning stage

Ceramic tapes were cut into shapes of the discs with diameter of 40 mm, then debinded and sintered using a conventional oven. The debinding and sintering were combined and a profile of this process is demonstrated in Fig. 8. At first, temperature is increasing from 25 °C till 500 °C with a ramp rate of 3 °C/min for approximately 2 h and 40 min. The reached temperature is stable for 1 hour. The second rise is from 500 °C till 1500 °C with the ramp rate of 3 °C/min for approximately 5 h 30 min. A dwell time at this temperature lasts for 2 hours. Finally, the temperature is decreasing from 1500 °C till 1450 °C with the ramp rate of 1 °C/min within 50 min and from 1450 °C till 50 °C with the ramp rate 3 °C/min for approximately 7 h 50 min. After that, samples of ceramic tapes

were collected from the conventional oven and cooled down to the room temperature. SEM analysis were done of those final products.

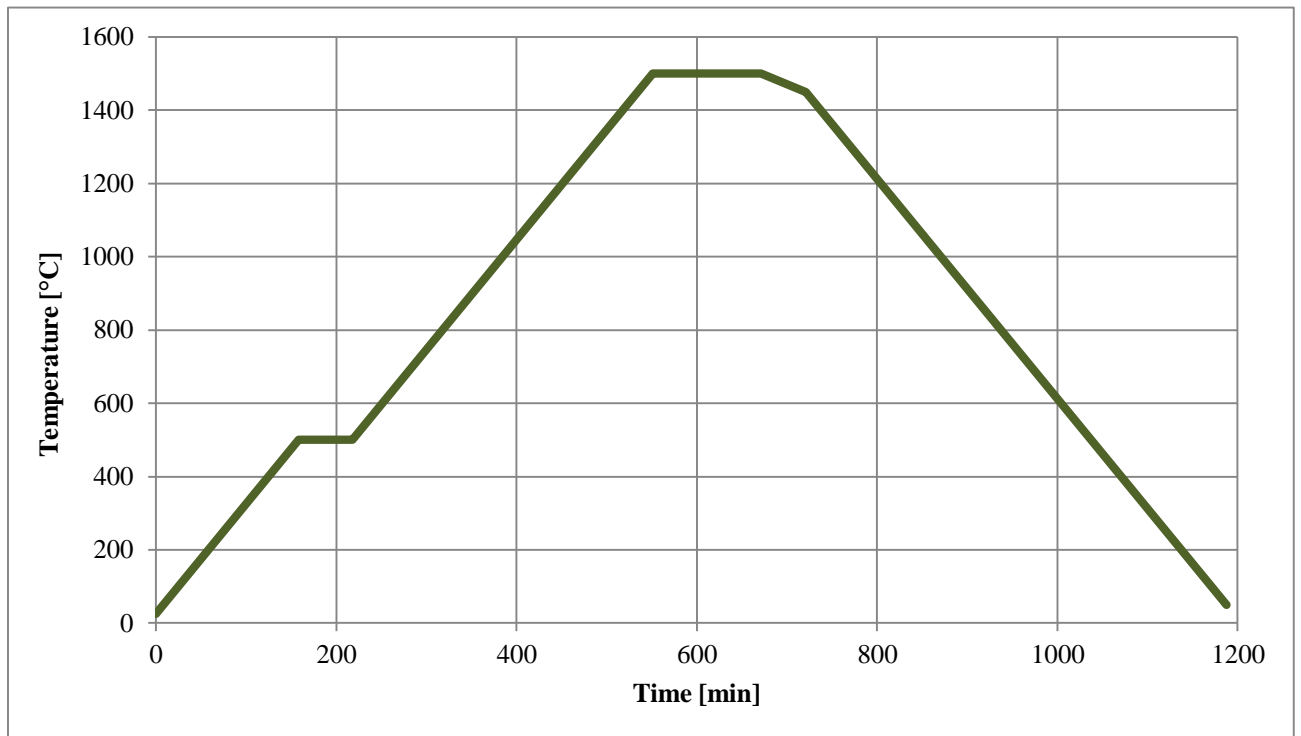


Fig. 8. Debinding and sintering profile of green tapes

2.3. Data analysis procedures

2.3.1. Potentiometric titration

Potentiometric titration was executed with *Zeta Probe* machine to investigate the IEP of zirconia dispersions. All dispersions were titrated from their natural pH in deionised water to the pH of 12 followed by back titration to the pH range of 2 – 3, using 0.1 M HCl and 0.1 M NaOH solutions at the room temperature.

For the measurements 150 ml dispersions with 5 wt % of zirconia and various wt % amounts (0.1 – 0.5 wt %) of DHC were prepared. Containers with dispersions were left for mixing on the roller bench for 24 h with speed of 50 rpm.

Data were analysed using *Zeta Probe* and *Microsoft Excel 2010* softwares.

2.3.2. Rheological characterization

Rheological characterization was executed with rotational rheometer *Modular Compact Rheometer MCR 302*. Each measurement cycle was repeated three times from 0.01 to 100 s⁻¹ with linear shear rate progression and shearing at constant rate of 0.01 s⁻¹ for 5 s and 50 s⁻¹ for 3 s. Measurements were carried out at 25 °C.

For the measurements 30 ml latex dispersions with different vol % amounts (10 – 50 vol %) of zirconia were prepared. Suspensions were put inside planetary mill jar with 5 mm zirconium oxide milling balls. The jar was placed in the planetary ball mill machine and milled in the circular motions for 10 min at 200 rpm before analysis. For samples with other additives, pore formers (10 wt % of zirconia) were added and milled for 2 min at 200 rpm.

Data were analysed using *Rheoplus* and *Microsoft Excel 2010* softwares.

2.3.3. FTIR

Analysis of the Fourier transform infrared spectroscopy (FTIR) was executed with *Bruker Tensor 27* spectrometer.

For the measurements slurries and tapes were prepared according to 2.2.2. and 2.2.3. procedures respectively. Samples of slurries and tapes were containing pore formers and also were done without them.

Data were analysed using *OPUS* and *Microsoft Excel 2010* softwares.

2.3.4. SEM

Analysis of the scanning electron microscopy (SEM) was executed with *Tescan SEM VEGA3* microscope to compare the microstructure of the sintered tapes.

For the surface investigation sintered samples were cutted into smaller pieces and placed on the graphite tapes, which were stucked to sample holders. For the cross section analysis, samples

were cut and placed between aluminium foil and screwed in the sample holders. Then they were coated with a thin gold-platinum layer using *Cressington Sputter Coater 108auto* at the vacuum of 0.02 mbar for 30 seconds.

Data were analysed using *VegaTC* software.

2.3.5. Archimedes' method

Analysis of the density was executed with *Mettler Toledo* balance and *Mettler Toledo RS-P42* printer by Archimedes' principle. The weight of the sample was measured in the air and in the liquid, while mercury was used as a liquid phase. All measurements were done two times.

For this investigation sintered samples were kept in the convectional oven at 100 °C for the overnight to liquidate humidity. After that, tapes were cut into smaller pieces for the measurement.

3. RESULTS AND DISCUSSION

3.1. Characterisation of dispersion

3.1.1. Selection of appropriate amount of surfactant

The zeta potential measurement helps to find the lowest amount of surfactant necessary for the efficient stabilisation of the dispersion. Using the potentiometric titration technique the amount of di-ammonium hydrogen citrate (DHC) was tested for the stabilisation of pure zirconia. These measurements were performed by 2.3.1. procedure.

Fig. 9 illustrates the relationship between zeta potential and pH of the YSZ dispersions without DHC and containing 0.1 – 0.5 wt % of DHC. The curve of YSZ dispersed in deionised water shows that the isoelectric point (IEP) is at 7.99. Below this value, the surface of positively charged particles adsorbs anionic surfactants due to electrostatic attractions [5]. By adding 0.1 wt % of DHC, the IEP shifts to more acidic region, at 5.44. Increasing the amount of surfactant, a change in the shape of curves is observed (with 0.2 – 0.5 wt % of DHC). First two curves are steep, while other curves are becoming more flat between pH range from 6 to 12, having similar zeta potential values, while pH is increasing till 12. This proves that zirconia is getting stabilised and the lowest amount of DHC to coat zirconia particles is around 0.2 – 0.3 wt %. To find the precise amount of surfactant, more potentiometric titration measurements using 0.125 – 0.275 wt % of DHC were done.

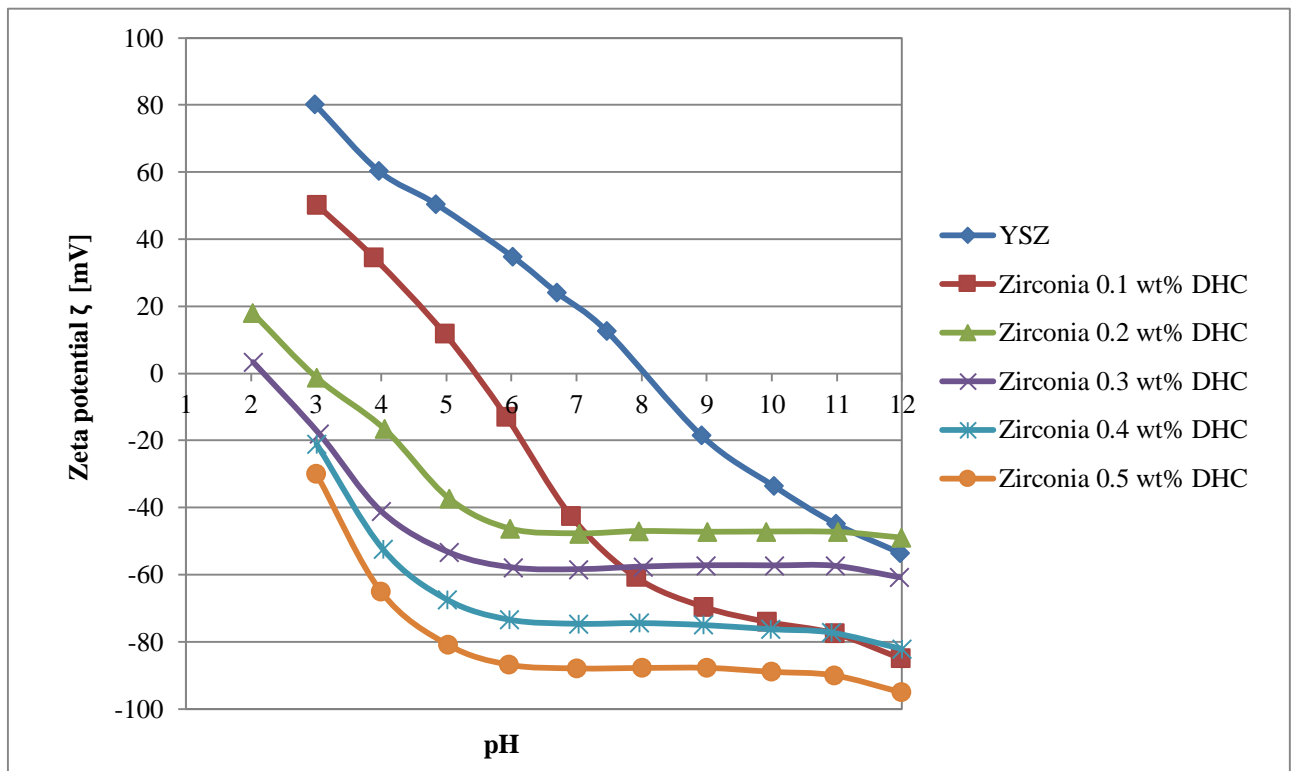


Fig. 9. Zeta potential versus pH of pure zirconia and zirconia with different amounts of DHC

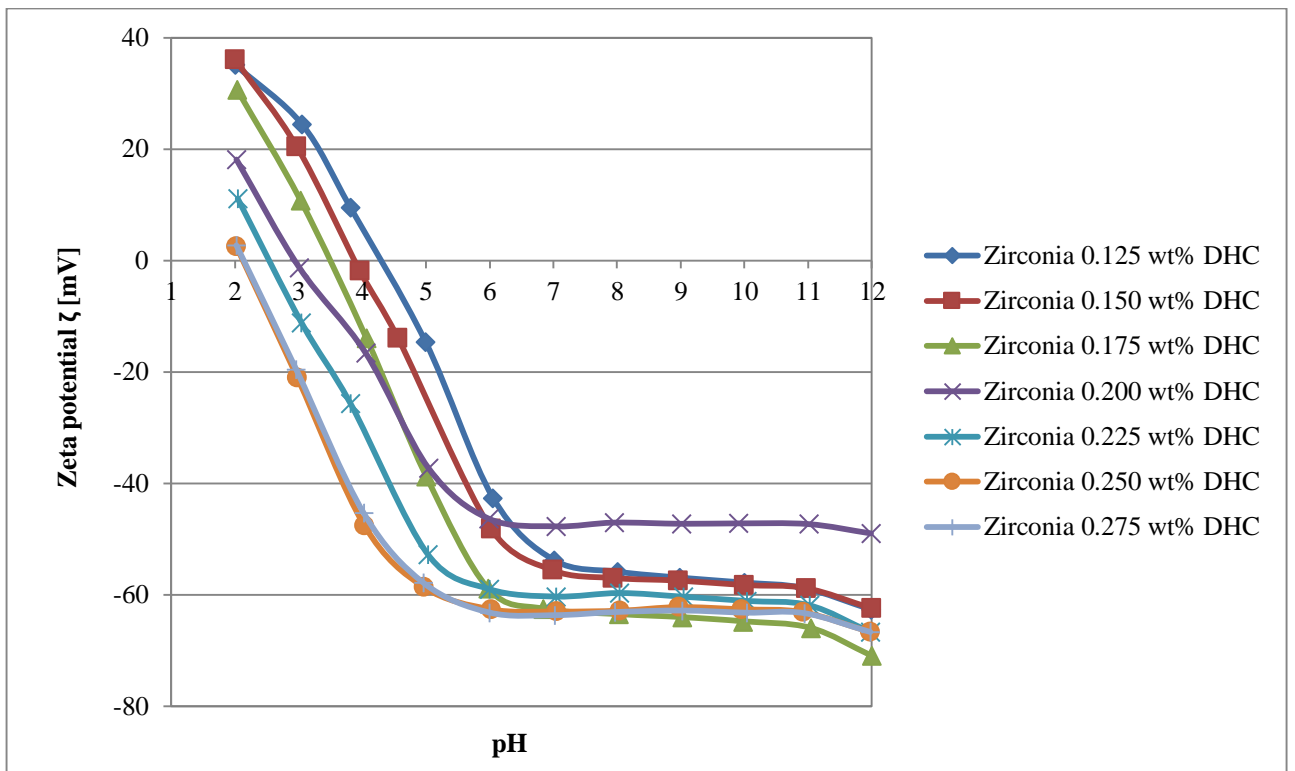


Fig. 10. Zeta potential versus pH of zirconia with different amounts of DHC

Fig. 10 presents the data of further zeta potential analysis. The addition of larger amounts of surfactant shifts all IEPs to lower values of pH from 4.28 till pH 2.16 and decreases the values of zeta potential. Nearly all curves have the same shape, when pH values are increased from 2 to 12. The curves representing zirconia with 0.250 wt % and 0.275 wt % of DHC are almost identical. To have a better view of the variation of IEP values, the graph showing IEP versus amount of DHC was presented (Fig. 11).

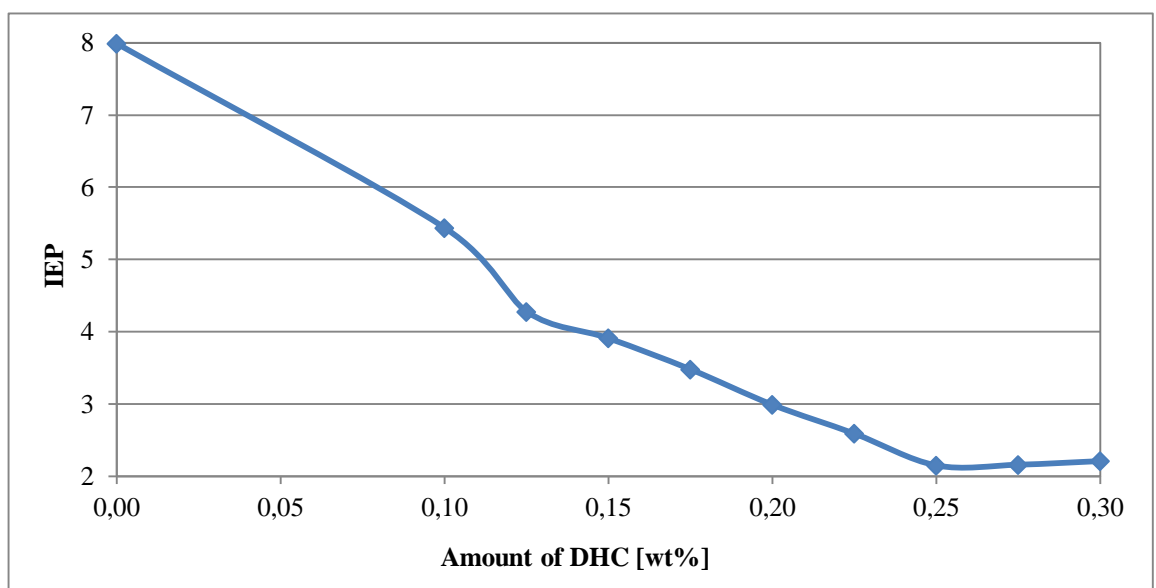


Fig. 11. IEP versus amount of DHC

By adding 0.125 wt % and 0.250 wt % of DHC to the dispersion, the values of the IEP decrease two and four times respectively. The relationship between the IEP and amount of DHC is almost linear. Although, when the dispersion has 0.250 wt % of DHC or more, a plateau has appeared. The first point of this plateau is the lowest amount of the surfactant, necessary for homogenising and stabilising zirconia powder. In further experiments, 0.250 wt % of DHC is used to obtain the stable homogenous dispersion.

3.1.2. Effect of solid load on viscosity values

Viscosity has significant influence on the tape casting process. The impact of the solid load in slurries was investigated by rheological analysis. The viscosity and shear stress behaviour while increasing shear rate was observed to find the highest possible amount of zirconia in the slurry composition. These measurements were performed by 2.3.2. procedure.

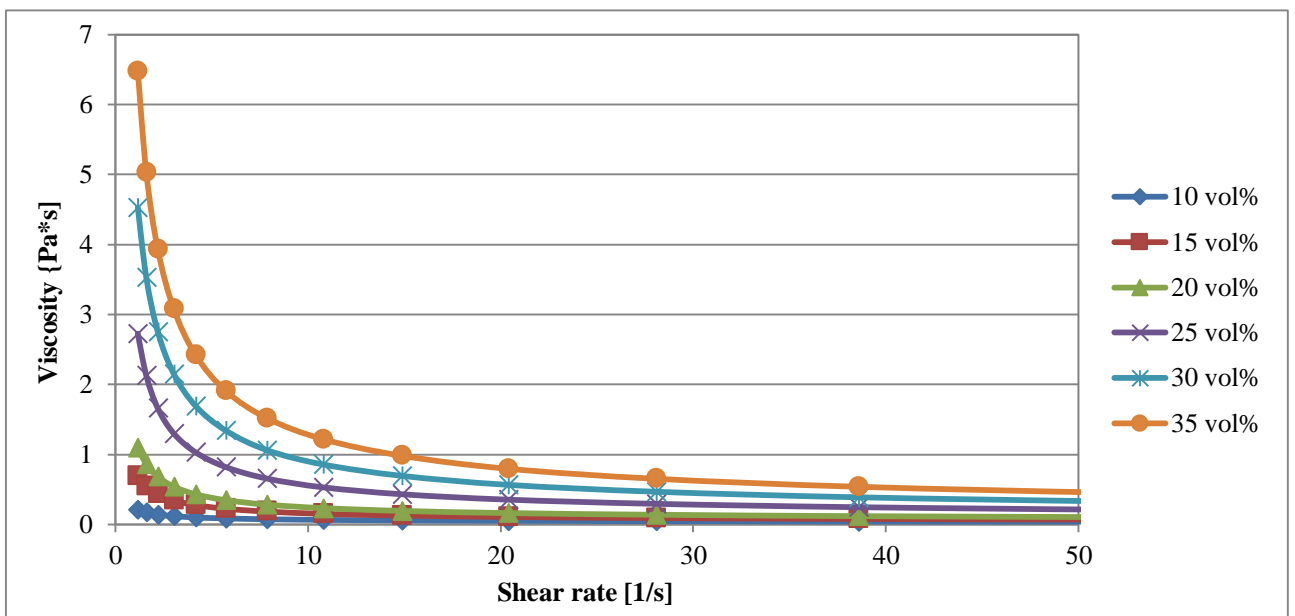


Fig. 12. Viscosity versus shear rate of the dispersions with the solid loads from 10 vol % to 35 vol %

Fig. 12 shows the influence of different solid loads on viscosity of the dispersions containing stabilised zirconia and binder only. While increasing the amount of zirconia in the dispersions, viscosity values are increasing respectively. At shear rate 1 s^{-1} , viscosity of the dispersion with the solid load 35 vol % is about 30 times higher than that of the dispersion with the solid load 10 vol %. The dispersion with the solid load 35 vol % is too viscous for the tape casting, thus the maximal solid load without agglomeration is 30 vol %. Dispersions with 10, 15 and 20 vol % solid loads have rather low viscosity values, lower than $1 \text{ Pa}\cdot\text{s}$ in the shear rate range $1 - 5 \text{ s}^{-1}$. When the shear rate is higher than 20 s^{-1} , viscosity of these dispersions is very low.

The dependence of shear stress on shear rate for the same dispersions is shown in Fig. 13. The values of the shear stress are increasing at higher shear rate and higher solid load. It is obvious from Fig. 12 and Fig. 13 that the optimal solid load is between 25 – 30 vol % of zirconia since it gives appropriate viscosity and shear stress for the slurry.

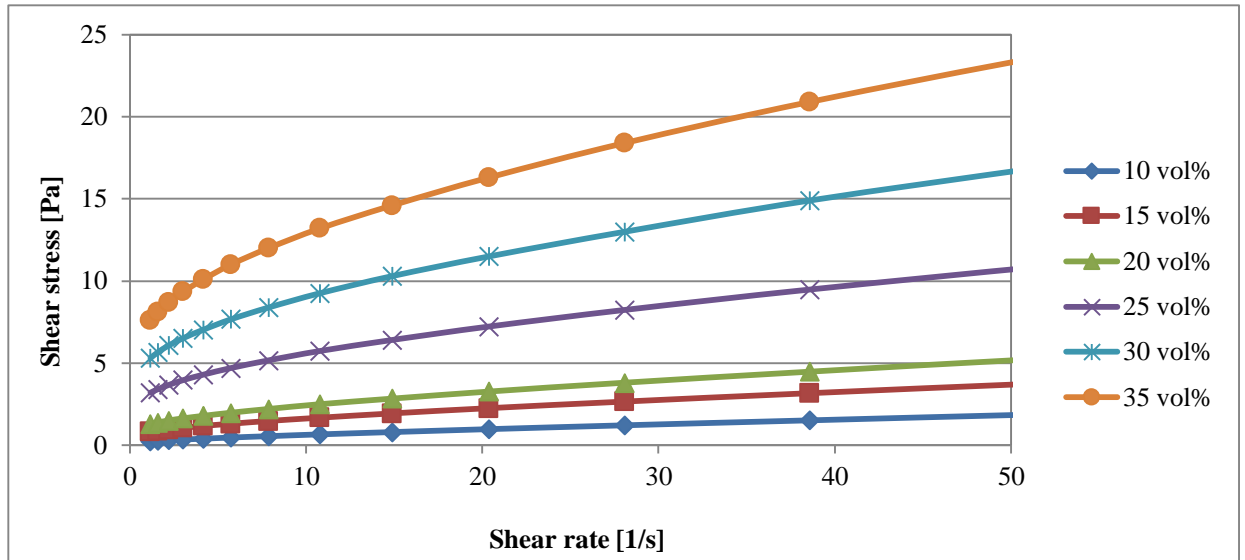


Fig. 13. Shear stress versus shear rate of the dispersions with the solid loads from 10 vol % to 35 vol %

In this thesis, the slurry for tape casting contains pore former (PF) – polystyrene dispersion in water. PF impacts the viscosity of the final dispersion by lowering it. Thus rheological measurements were done with the samples containing zirconia (25 – 45 vol %) and PF (10 wt % of zirconia).

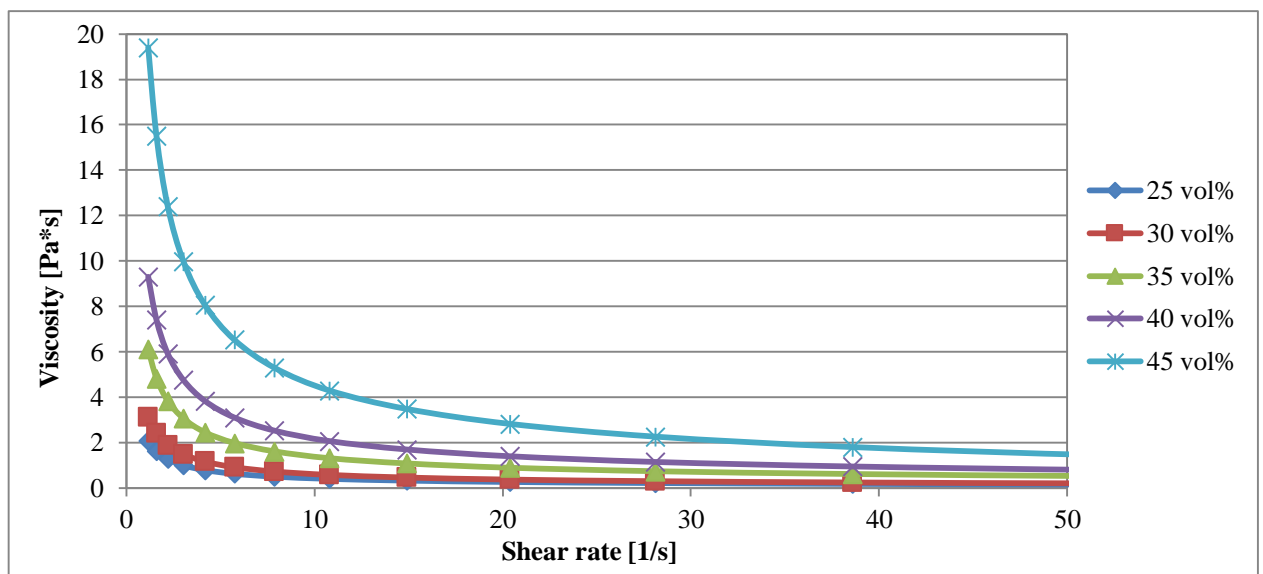


Fig. 14. Viscosity versus shear rate of the dispersions with the solid loads from 25 vol % to 45 vol % containing pore former DPP 3710 (10 wt % of zirconia)

Fig. 14 presents viscosity of the dispersions containing PF versus shear rate. The dispersions differ slightly in their compositions, and their viscosities are rather different. Like in Fig. 12, viscosity is going down with increasing shear rate, and reaches almost constant level at shear rate at about 40 s^{-1} . The dispersion with the solid load 40 vol % is pasty and shows agglomeration behaviour, thus it is not suitable for the tape casting. The maximal solid load for the ceramic tapes manufacturing with pore structure is 35 vol %.

Fig. 15 illustrates the relationship between shear stress and shear rate of dispersions containing PF. An increase in the solid load resulted in higher shear stress. In the shear rate range $1 - 10 \text{ s}^{-1}$, the values of the shear stress are low but they increase when the shear rate is getting higher. An exception is the curve, which presents the dispersion containing 45 vol % of zirconia. It looks steep at the beginning showing fast increase in the shear stress.

The most suitable solid load is 30 vol % and it has been used for the further experiments. The viscosity and shear stress values of this dispersion is complementary to the sample with 25 vol % of zirconia without PF and fits in the limits of the viscosity, which were determined during analysis without PF.

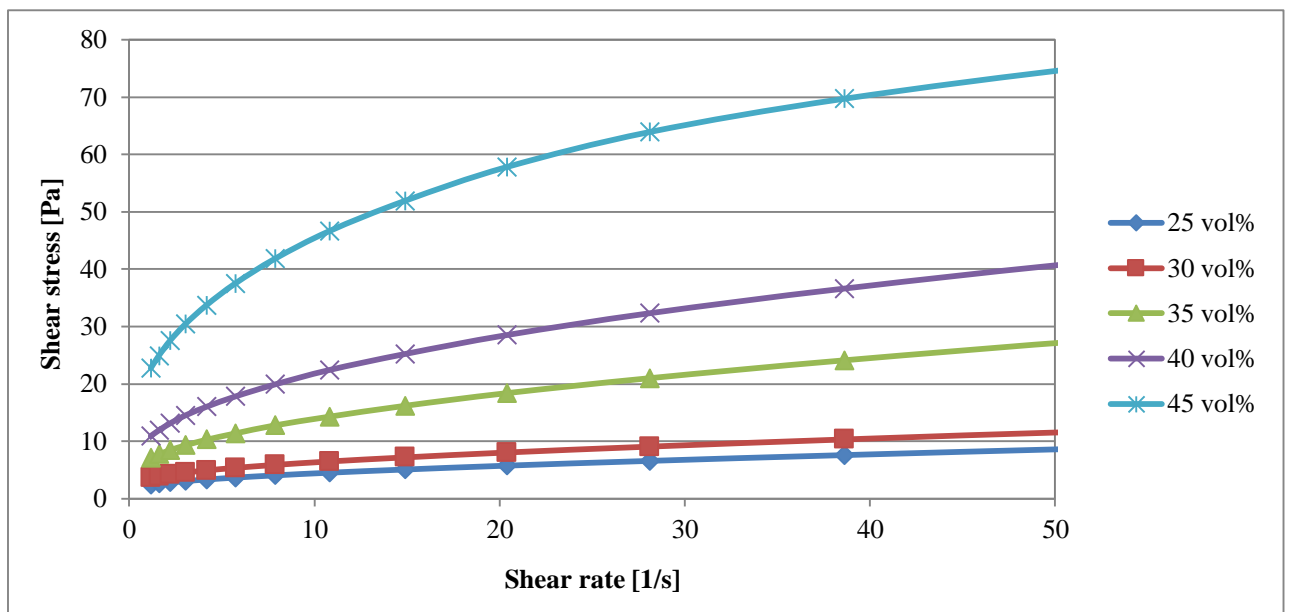


Fig. 15. Shear stress versus shear rate of the dispersions with the solid loads from 25 vol % to 45 vol % containing pore former DPP 3710 (10 wt % of zirconia)

Figures 12-15 confirm that all zirconia dispersions possess shear thinning behaviour, which increases with solid loading. The viscosity depends on the shear stress behaviour, thus pseudoplasticity is required for the tape casting. During production of the tapes, the pseudoplastic slurry passes under the casting blade, and the viscosity significantly decreases. When the slurry is dragged out of the casting unit, which prevents the slurry from flowing aside and keeps the shape of

the formed tape, the viscosity values increase to suppress uncontrolled flow and to prevent sedimentation of the ceramic particles [1, 6].

3.2. Characterisation of UV curing system

3.2.1. UV induced free radical photopolymerisation of the latex binder

The slurry was prepared according to 2.2.2. procedure. The tape casting and UV curing stages were held by 2.2.3. procedure. Fig. 16 illustrates a simplified scheme of the UV induced free radical photopolymerisation, when urethane acrylate dispersion is used as a binder and 2-hydroxy-2-methyl-1-phenyl-1-propanone as a photoinitiator. At the initiation stage, the photoinitiator is activated by the UV light and splits into two radicals. The radical which has a bigger activation energy reacts to a stump of the acrylic acid. Then, radicals on growing polymeric chain attack double bonded monomers by creating growing polymeric net due to more than one acrylic group in the latex particle. There is no information how many acrylic acid stumps has one latex particle. Although, the provider gives the data that the amount of esters with acrylic groups is between 5 – 15 wt %.

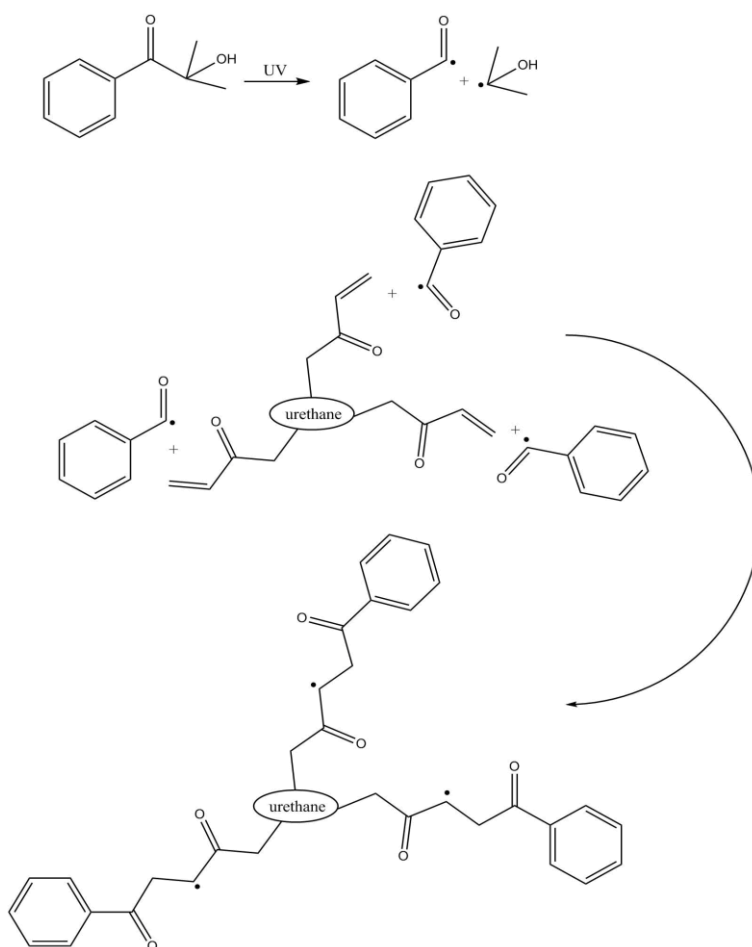


Fig. 16. Scheme of the UV induced free radical photopolymerisation using urethane acrylate dispersion and 2-hydroxy-2-methyl-1-phenyl-1-propanone

Fig. 17 presents FTIR spectrum before and after UV irradiation. This analysis was done by 2.2.2. and 2.3.3. procedures to confirm the photopolymerisation process and to see if an addition of pore formers has significant changes during the photopolymerisation process. Peak in the region of $1750 - 1650 \text{ cm}^{-1}$ characterise a carbon-carbon double bond of the acrylate. Some changes in the region of $1500 - 1550 \text{ cm}^{-1}$, which is also responsible of the carbon-carbon double bond, are visible too. After the photopolymerisation, the absorbance in those regions gets lower, comparing to the uncured slurry and proves that the photopolymerisation is happening during the UV treatment. Decrement of the absorbance after the UV curing is from 0.31 % to 0.10 %, when no pore formers are in the composition. Although, if the tape contains pore formers this decrement is not so significant – from 0.20 % to 0.16 %, so a monomer conversion to the polymer is rather low. This could be explained that pore formers blocks growing polymeric chains by not letting them to move freely. Radicals on those chains can not attack double bonds and after UV curing there are lots of monomers left. The minor conversion of the monomers could have an influence of the mechanical properties of the ceramic tapes by lowering their strength.

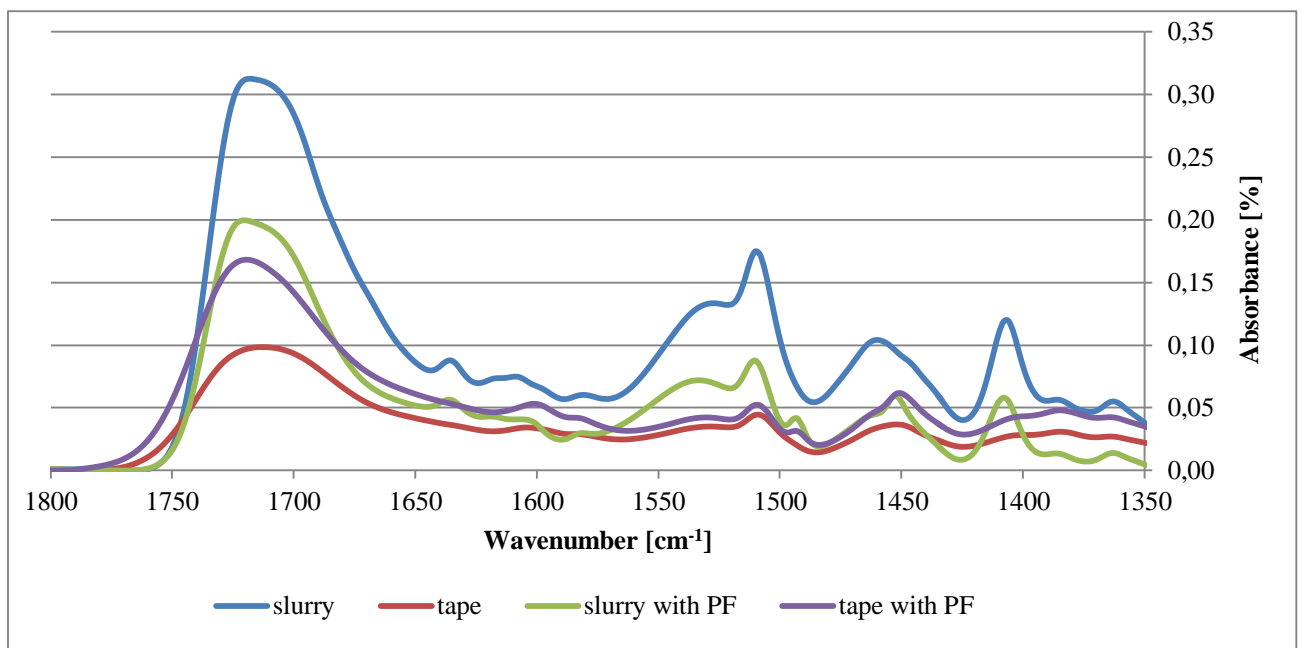


Fig. 17. FTIR spectrum of the slurries before UV curing and of the tapes after UV curing

To assure that no water is left through the whole thickness of the tape after the UV curing, variations of the weight were observed. Tapes were weighted before and after the UV curing. When the photopolymerisation stage was finished, tapes were 10 – 12 % lighter. After 1, 2, 4 and 8 hours the weight of cured samples was the same. It did not changed even after a week. This means that in the UV curing box all water have been evaporated and tapes are completely dry.

3.2.2. Selection of appropriate amount of photoinitiator and UV curing time

The investigation of the UV curing system was done by finding the lowest amount of the photoinitiator and the shortest UV curing time to produce quality green tapes. For this experiment the slurry was prepared according to 2.2.2. procedure with different amounts of the photoinitiator – from 1 to 4 wt % of latex binders. The tape casting and UV curing stages were held by 2.2.3. procedure by shaping one layer, whose theoretical thickness was 150 μm . The time of photopolymerisation mediated from 20 to 45 minutes.

Table 1. Quality of the green tapes with different amounts of the I and various UV curing times.

I, wt% of binder	UV curing time, min					
	20	25	30	35	40	45
1.0	-	-	-	-	×	×
1.5	-	-	-	×	×	×
2.0	-	-	2.0-30	2.0-35	×	×
2.5	-	2.5-25	2.5-30	2.5-35	×	×
3.0	-	3.0-25	3.0-30	3.0-35	×	×
3.5	-	3.5-25	3.5-30	3.5-35	×	×
4.0	-	4.0-25	4.0-30	×	×	×

Table 1 presents results of this investigation. Fields with a dash (-) mean that tapes with that particular amount of the photoinitiator and UV curing time after this experiment were wet and not photopolymerised. Fields with a cross (×) show which tapes were cracked after UV curing and were not suitable for further debinding and sintering stage. Green and orange colours show with which curing system it is possible to get good quality green tapes. Tapes were named by the specific system. The first number means the amount of the photoinitiator and the second number shows the duration of the UV curing. Although, some of tapes cured for 35 minutes with the different amount of the photoinitiator distinguished in cracks. The best quality tapes were debinded and sintered according 2.2.4. procedure to see an impact of the thermal treatment and to analyse microstructure using SEM technique.

Fig. 18 shows the quality of green tapes before the burning stage. All tapes were bended to check their flexibility. Also, discs were cut and removed to see a cohesion between ceramic tape and polyester film. Tapes, which are marked with letters *a* and *b*, are flexible and easy to remove. Samples *c* and *d* present tapes, which distinguished in cracks after bending and were non removable from the polymeric substrate without damaging it.

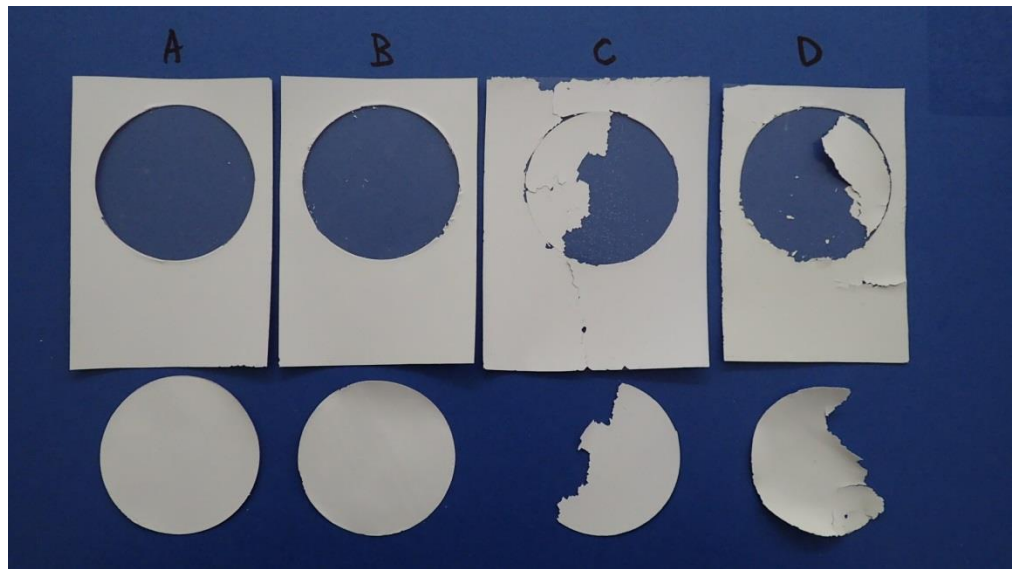


Fig. 18. Illustration of the quality of the green tapes: (a) 2.5-30, (b) 3.0-30, (c) 1.5-45, (d) 3.0-45

Fig. 19 presents the quality of sintered samples. Flat and solid tapes were expected after debinding and sintering. Although, curling behavior were observed in all one-layered sintered samples (*a-c*). The thicker tape with two layers (*d*) was flat. Sample *a* present an appearance of the solid tape, sample *b* – the cracked tape and sample *c* – the collapsed tape, which is not suitable for the further analysis. The best quality tape after the burning stage was 2.5-30.

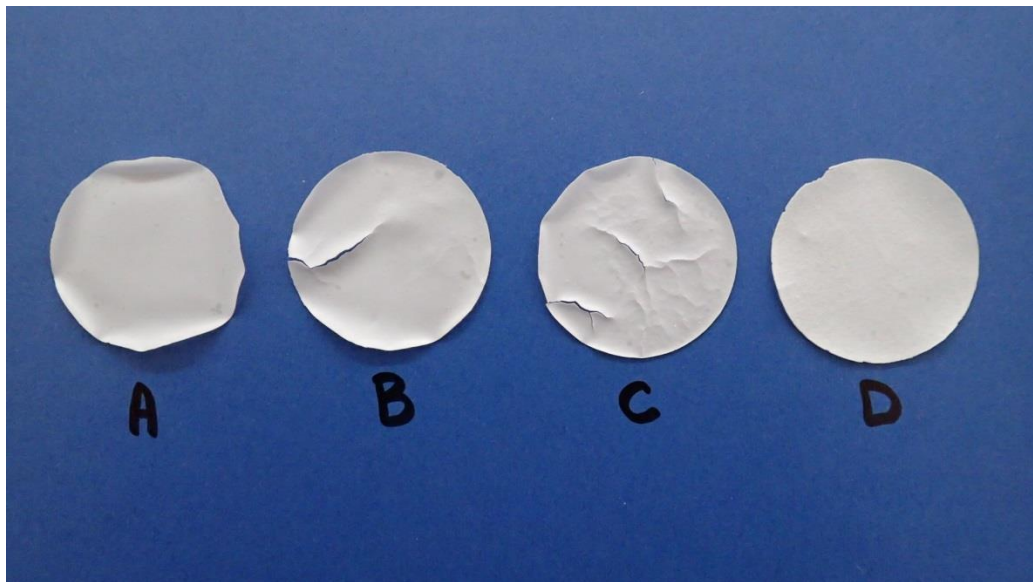


Fig. 19. Illustration of the quality of the sintered tapes: (a) 2.5-30, (b) 4.0-25, (c) 3.5-30, (d) 3.0-30

According to 2.3.4. procedure the microsurface of ceramic tapes was examined. On all samples it was possible to distinguished air bubbles and some of them had microcracks. In Fig. 20 different types of defects are shown. SEM pictures a and b presents consequences of major air bubbles after debinding and sintering with different magnifications. They form a hole and some

cracks while tape is thermal treated. The minor air bubble leaves just the small hole (marked this a red circle) without any slots as in the sample *c*.

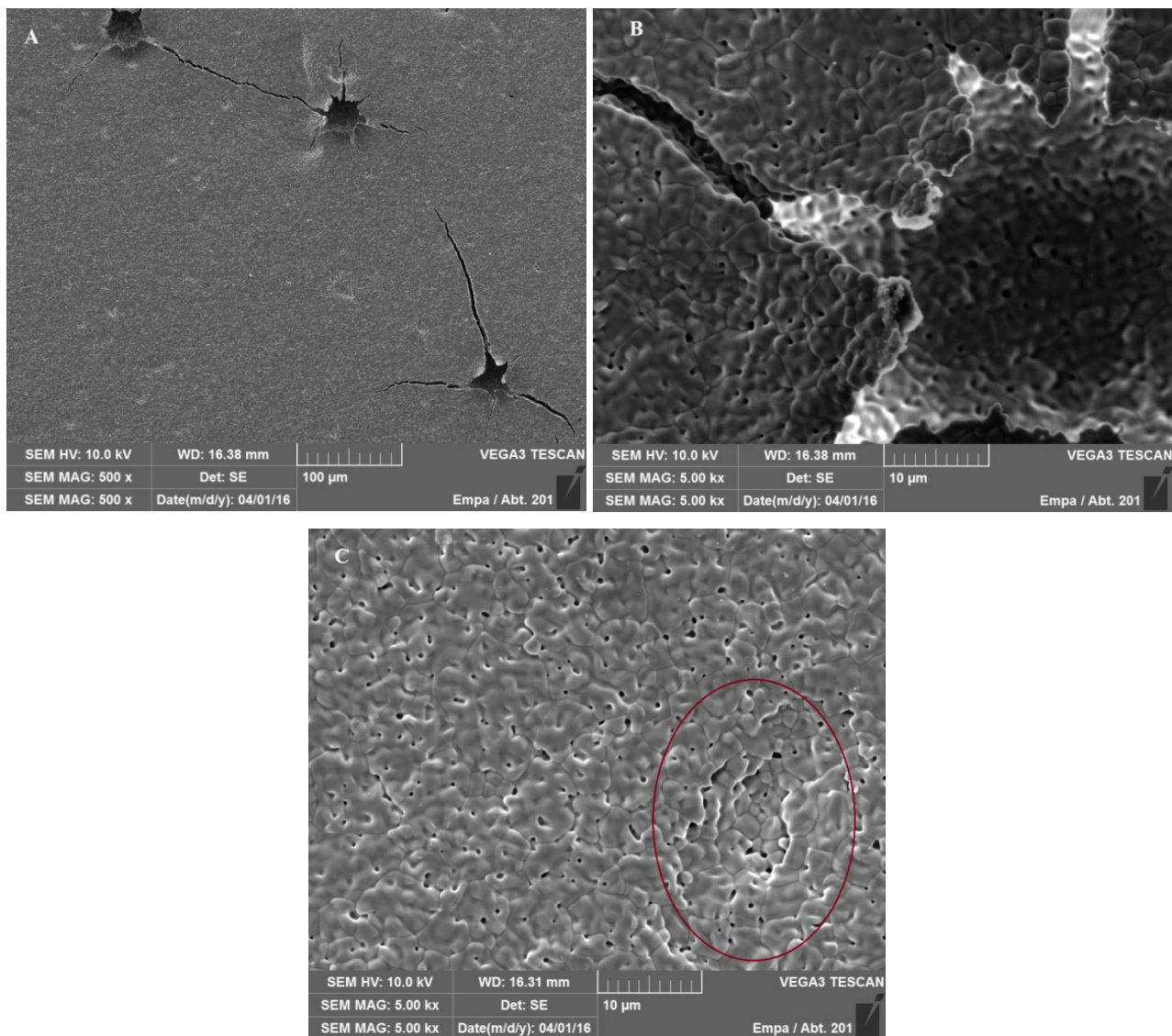


Fig. 20. SEM pictures, which are showing air bubbles in tapes after thermal treatment: (a) 2.5-25, (b) 2.5-25, (c) 2-30

To remove air bubbles, 1-octanol was used as a defoaming agent. 0.5 wt % of 1-octanol, according to the sum of masses of the powder and binder, was added after mixing in the planetary ball mill machine. With higher concentrations of the defoaming agent, slurries were showing dewetting behaviour on the substrate, while being tape casted. Less than 0.5 wt % – were not efficient enough. Besides, different ways of additions were checked to optimise the degasing process. 1-octanol was added to the slurry composition in three ways – before first mixing, when the powder and binder are added; before last mixing, when the photoinitiator is added; after the tape casting process, without any mixing in the planetary ball mill machine. The best results were achieved with the first way. Using the third – a lack of the homogeneity was observed.

3.3. Characterisation of the sintered tapes

In this chapter, characteristics of the sintered tapes are presented. Shrinkage, which is the change of the volume without removing parts of the material or pressing. Microstructure of the surfaces and cross-sections to identify the quality of the ceramic tapes. Density and porosity values, which are important for the application of the tape casted products.

The theoretical thickness of all one layered tapes was 150 μm . It was possible to get two layers when the gap of the doctor blade for the first layer during tape casting was 150 μm and second – 200 μm , as well as three layers, while the first layer was 100 μm , second – 150 μm and third – 200 μm . Tapes consisting of four or more layers were starting to curl and cracks on the surface were visible with the naked eye.

3.3.1. Shrinkage

The shrinkage was geometrically measured after UV curing and thermal treatment processes. The results of the shrinkage were the same even when sintering profile where changed by lowering sintering temperature from 1500 $^{\circ}\text{C}$ to 1300 $^{\circ}\text{C}$ and, after 2 hours of dwell in this temperature, decreasing it from 1300 $^{\circ}\text{C}$ till 900 $^{\circ}\text{C}$ with the ramp rate of 1 $^{\circ}\text{C}/\text{min}$. Although, when this sintering temperature was switched to 1150 $^{\circ}\text{C}$, a significant changes in the shrinkage were observed. Fig. 21 shows that the differences in the shrinkage in the diameter, while having various sintering temperatures, can be easily seen without measuring. Tapes in this illustration are named with sintering temperature and another temperature, which is reached at the first cooling step. Also, the quality of the tape is better with the lowest sintering temperature (*c*). All samples after this thermal treatment profile were flat and without cracks.

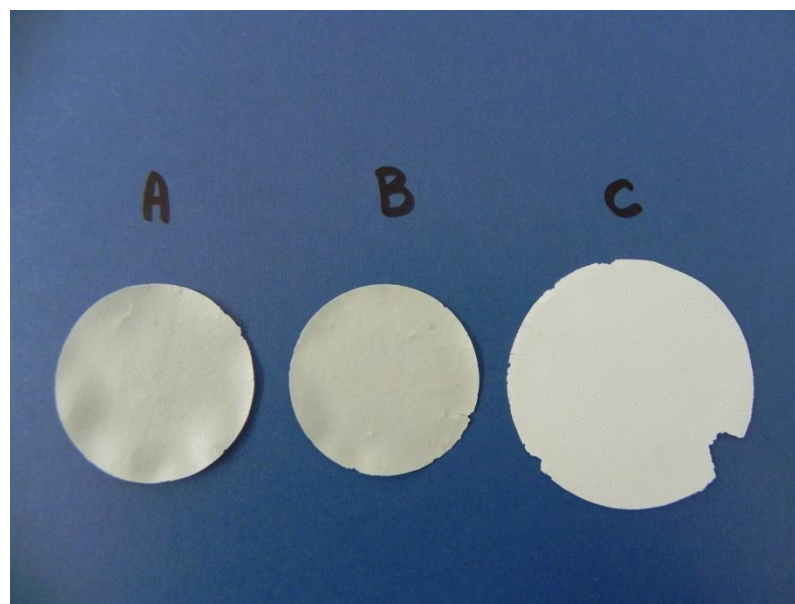


Fig. 21. Illustration of the shrinkage in the diameter: (a) 1500-1450, (b) 1300-900, (c) 1150-900

Thus, when sintering temperature is 1500 °C or 1300 °C, the shrinkage in the diameter is 25 % for one, two and three layered tapes. Decreasing temperature till 1150 °C, the obtainable shrinkage is ten times less – 2.5 %. Values of the shrinkage in the thickness direction are different for all layers. Heating one layered samples at 1500 °C or 1300 °C, the shrinkage mediates from 5.5 to 6.5 %, two – from 3 to 3.5 % and three – from 2.5 to 3 %. After sintering at 1150 °C, one layer shrinks 15 %, two – 12 % and three – 9 %.

3.3.2. Microstructure of the tapes sintered at 1500 °C and 1300 °C

After debinding and sintering ceramic tapes were characterised with SEM technique according to 2.3.4. procedure. In this subsection results of sintering at 1500 °C and 1300 °C are presented by SEM pictures of surfaces and cross-sections.

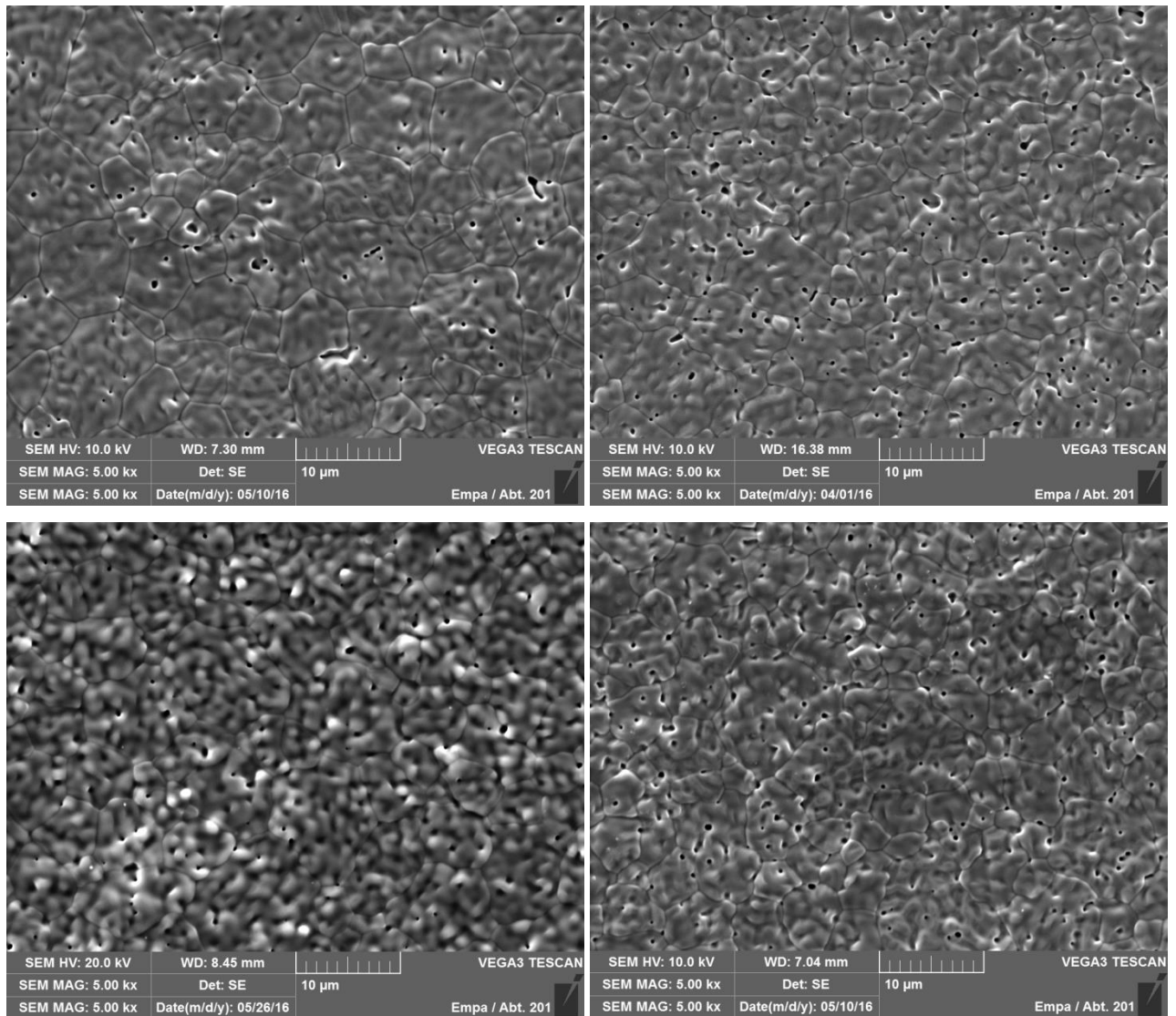


Fig. 22. SEM pictures of the tapes sintered at 1500 °C: (top left) without PF, (top right) with 140 nm PF, (bottom left) with 260 nm PF, (bottom right) with 450 nm PF

At first, one layered tapes were done with different pore formers and various amounts of them in the slurry composition, counted by the total solid loading – 2.5, 5, 10 and 15 wt %. The highest possible amount of PF was 10 wt % and this percentage was chosen for further experiments. After the UV curing, tapes with 15 wt % of PF distinguished in lots of cracks and when the burning stage was done, they were too fragile.

In Fig. 22 the surface microstructure of tapes sintered at 1500 °C are presented. SEM picture of the surface of these one-layered tapes shows ceramics without cracks, air bubbles or other defects. Although, some singular holes after air bubbles were found on the sample surface during SEM analysis. In the picture showing the tape without the addition of PF during manufacturing, some pores are visible. They could be created by the latex binder, while it was burned out in the oven. Porosity seems higher in other pictures, but the size of pores looks the same. Using a higher magnification, no pores less than 450 nm were spotted.

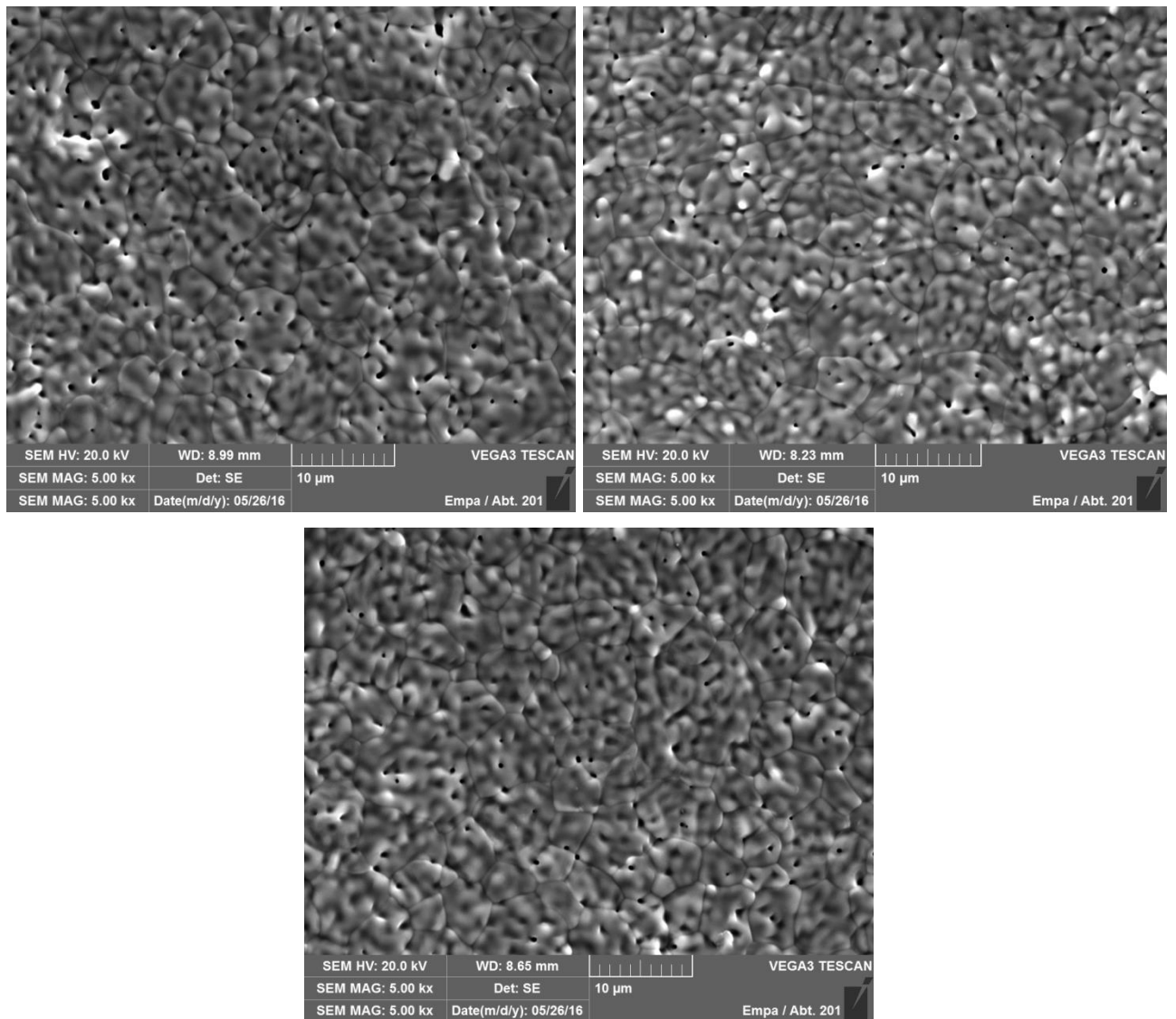


Fig. 23. SEM pictures of tapes sintered at 1300 °C: (top left) with 260 nm PF, cooled to 1100 °C; (top right) with 260 nm PF, cooled do to 900 °C; (bottom) with 450 nm PF, cooled to 900 °C

The sintering temperature and the first cooling down have an important role in the microstructure of tapes. High temperature will lead to dense product. During sintering, a thermal conductivity in the sample is a bit higher than in the oven. Due to contrasts of the temperatures in the different areas of the tape, the slow cooling after sintering is necessary. Otherwise, ceramics will distinguish in cracks and bad quality.

It was decided to lower sintering temperature till 1300 °C and then to cool down to 1100 °C and 900 °C, to see if a bigger subtraction of these temperatures has noticeable influence in the microstructure of tapes. Results of this experiment are presented in Fig. 23. It is hard to see the difference of porosity, while having different cooling temperature (pictures above) and PF (above left and below), as well as, to compare them with previous results in Fig. 22. For this, further experiments of density and porosity of tapes are presented in the subsection 3.3.4.

The view of the surface area is not the only importance during SEM analysis, when tapes have a multilayered structures. Cross-sections must to be studied to see if there is any delamination. Besides, in this thesis a gradient structure was wished to design by creating the first layer without PF in the slurry composition, while the second and third were manufactured with different PF.

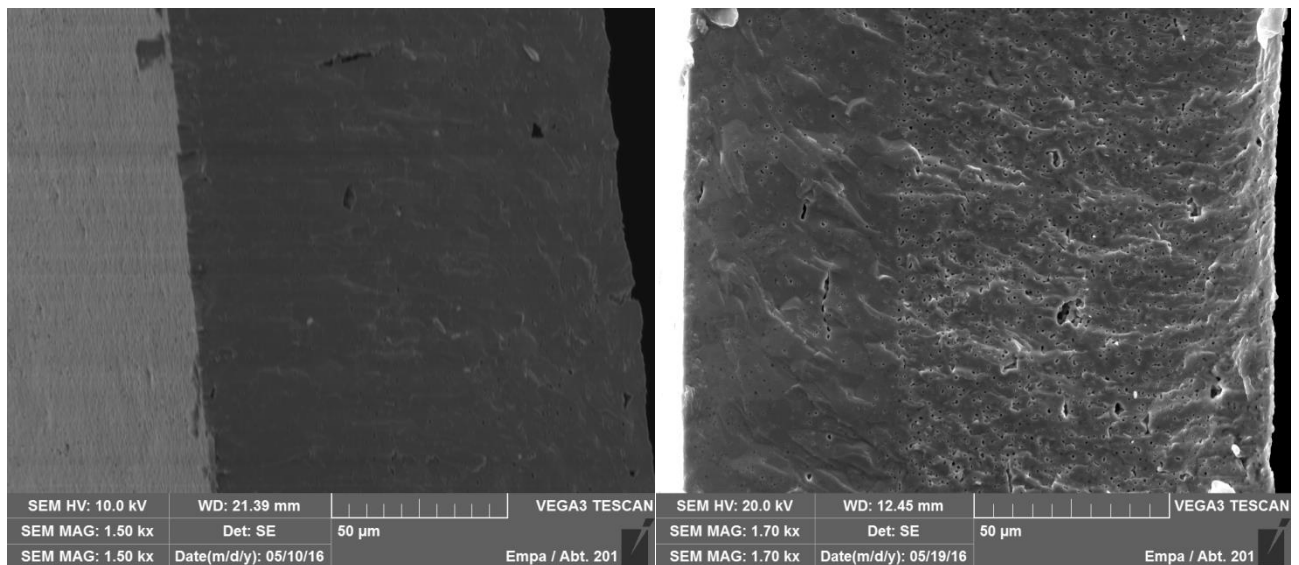


Fig. 24. SEM pictures of cross-sections of the tapes sintered at 1500 °C and 1300 °C: (left) 2 layers without PF, sintered at 1500 °C; (right) 2 layers – w/o, 540 nm PF, sintered at 1300 °C

In Fig. 24 pictures of cross-sections are presented. The picture on the left shows 2 layers produce without PF. The darker side is the cross-section and the lighter side is the surface of this sample. No delamination is visible. Although, it is impossible to know where an interface between two layers is. For this reason, two layered tape, in which the first layer is without PF and second was casted with 450 nm PF, is showed. As in the previous picture, two clearly visible surfaces have no delamination and the gradient structure is observed.

3.3.3. Microstructure of the tapes sintered at 1150 °C

Another experiment with the sintering temperature was done. 1150 °C were chosen for the heating for 2 hours and cooling down till 900 °C, with a ramp rate 1 °C, as always. Fig. 25 shows SEM pictures of three-layered tapes. These tapes compared to previous results, which were presented in the subsection 3.3.2., are highly porous. Also, the grain size are much more smaller. The gradient structure could not be seen, because of high porosity. Some photos which higher magnification were taken, although they were not quality enough. At this sintering temperature, ceramic tapes without any major defects and delamination are observed.

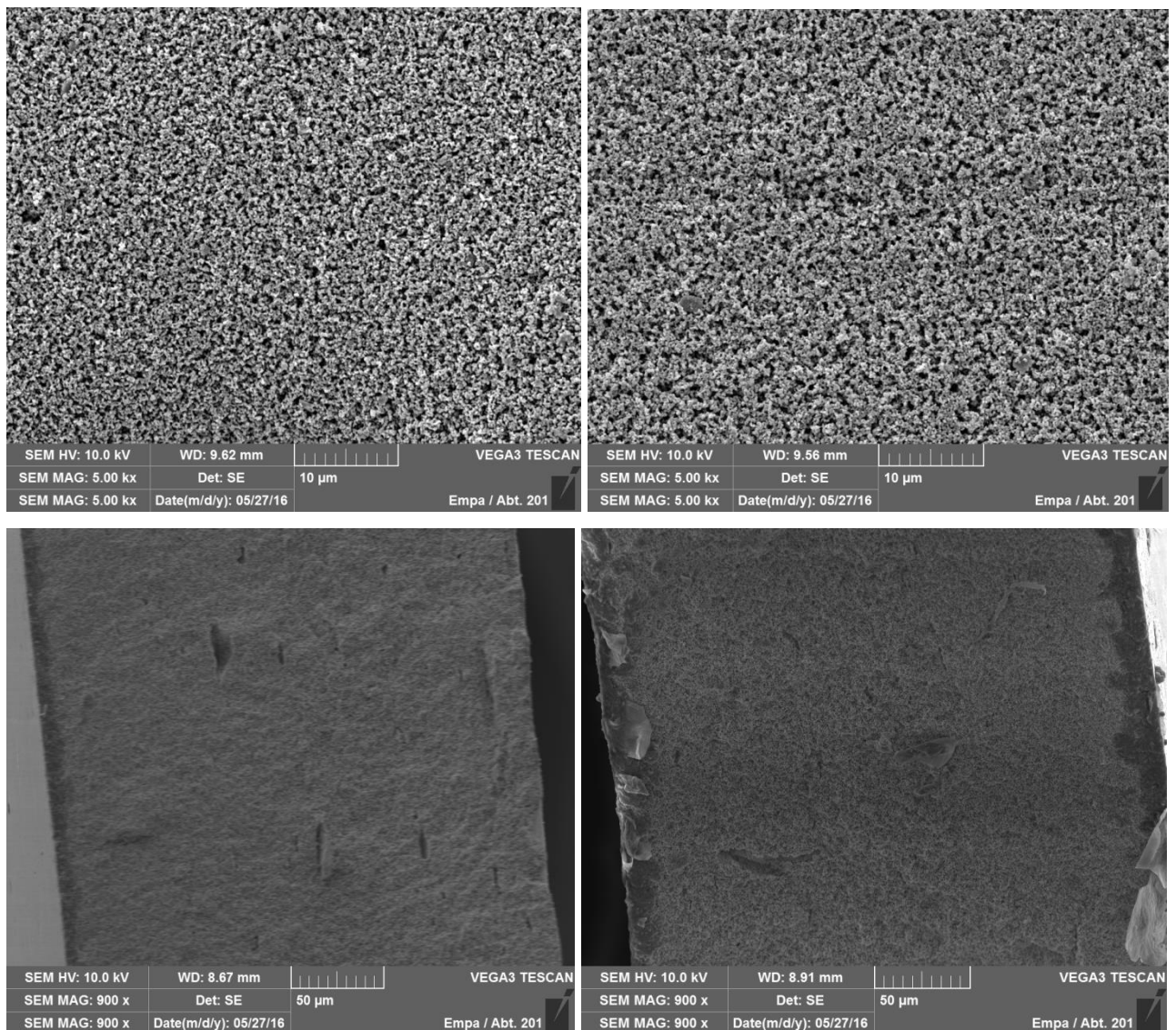


Fig. 25. SEM pictures of the sintered tapes at 1100 °C: (top left) surface of three layers – w/o, 140 nm PF, 260 nm PF; (top right) cross-section of three layers – w/o, 140 nm PF, 260 nm PF; (bottom left) surface of three layers – w/o, 260 nm PF, 450 nm PF; (bottom right) cross-section of three layers – w/o, 260 nm PF, 450 nm PF

While analysing SEM pictures the quality of tapes and sizes of particles could be observed. Although, the difference between sintering temperatures cannot be compared correctly. Besides, smaller pores could not be seen because the microscope is not powerful enough. To have a better understanding of the influence of sintering temperatures, other analysis are needed.

3.3.4. Density and porosity

To investigate bulk and apparent densities, pore diameter and total porosity percentage, analysis of the mercury intrusion porosimetry (MIP) was executed with *Pascal 140/440* porosimeter. Measurements of the different one layered tapes were done with maximum pressure of 200 MPa, mercury surface tension 0.48 N/m and contact angle of mercury 140°. For this investigation sintered samples were kept in the convectional oven at 100 °C for the overnight to get ride of humidity. After that, tapes were cut into smaller pieces for the measurement. Although, during this analysis density and porosity parameters were not evaluated appropriately due to fragileness of the samples while having high pressure in the measuring system. For this reason it was decided to measure the density using Archimedes' method (2.3.5. procedure).

Table 2. Density and porosity results of different tapes.

Sintering type	I layer	II layer	III layer	Density, g/cm ³	Porosity, %
1300-1100	w/o	140 nm	-	5.28	11.71
		260 nm		5.22	12.71
		450 nm		4.97	16.89
1300-900	w/o	140 nm	-	5.10	14.72
		260 nm		5.10	14.72
		450 nm		4.91	17.90
		140 nm	260 nm	5.16	13.71
		260 nm	450 nm	4.66	22.03
1150-900	w/o	140 nm	-	2.37	60.37
		260 nm		2.39	60.03
		450 nm		2.19	63.38
		140 nm	260 nm	2.48	58.53
		260 nm	450 nm	2.20	63.21

Results of this investigation are presented in the Table 2. Tapes with three different sintering types were characterised – when the sintering was held at 1300 °C and the first cooling was till 1100

°C and 900 °C, as well as, the best thermal treatment for tapes from 1150 °C to 900 °C. The first layer of all tapes is without pore formers, while the slurry for the second and third layer casting had PF.

Density of tapes is decreasing, when second or third layers have been produced with bigger PF. The relationship of porosity and the size of PF is opposite – it is increasing. While manufacturing ceramic tapes, 140 and 260 nm PF are used, analysed parameters are more or less the same. Although, these results are a bit higher with 450 nm PF. This could be explained that smaller pores are being destroyed during thermal treatment. But intergranular porosity (space between grains of the ceramic powder) is still observed in samples, where 140 and 260 nm pores were planned. The provement of this statement can be the comparison of density and porosity results with different sintering temperatures. When the highest heating point is 1300 °C, tapes are more dense, from 4.66 till 5.28 g/cm³, then sintered at 1150 °C – from 2.19 to 2.48 g/cm³. Besides, the temperature of the first cooling has an influence. Changing it from 1100 °C to 900 °C, decreases density in tapes. Thus, porous structure was observed with the lowest sintering temperature and the highest tapes in porosity were two- and three-layered with PF of 450 nm size – 63.38 and 63.21 % respectively.

Conclusions

1. To obtain stable homogenous zirconium oxide dispersion, the lowest amount of diammonium hydrogen citrate as the surfactant is 0.250 wt %.
2. Compatibility between water based UV curable binder and water based pore formers have been proved.
3. The appropriate solid load in the ceramic slurry is between 25 – 30 vol %. When pore formers (10 wt % of ZrO_2) are used, the highest possible solid load is 30 vol %. All dispersions possess the shear thinning behaviour.
4. FTIR spectrum proves photopolymerisation process. Although, usage of pore formers lowers the conversion of the monomer during UV curing. The best quality green tapes and sintered samples were observed using 2.5 wt % of the photoinitiator and 30 minutes of the UV curing process.
5. When the sintering temperature was 1500 °C and 1300 °C, all tapes have shrunk 25 % in the diameter. The shrinkage in the thickness direction for one layer tapes was from 5.5 to 6.5 %, two – from 3 to 3.5 % and three – from 2.5 to 3 %. With the sintering temperature of 1150 °C, all tapes have shrunk 2.5 % in the diameter. The shrinkage in the thickness direction for one layer tapes was 15 %, two – 12 % and three – 9 %.
6. Highly porous, small grain size zirconia ceramics with the gradient structure were observed when the sintering temperature was 1150 °C. It was possible to get two- and three-layered structures without delamination.
7. Density of tapes decreases and porosity increases with lower sintering temperature and 450 nm pore formers. The highest porosity was 63.38 %, when the tape was two-layered.
8. It is possible to use tape casting technique with fully water based system – binders and pore formers.
9. Further investigations concerning smaller sizes of pore formers could be done including further studies of the sintering behavior.

SANTRAUKA

Plėvelių liejimas yra nebrangi ir plačiai naudojama technika, siekiant sukurti plonas keramines juosteles, pasižyminčias daugiasluoksne struktūra. Plėvelės formuojamos iš dispersijos, kurią sudaro keraminiai milteliai ir organiniai priedai (stabilizatoriai, rišikliai, plastifikatoriai, fotoiniciatoriai), būtini siekiant joms suteikti gerą koheziją ir lankstumą. Dispersijos terpė gali būti sudaryta iš įvairių organinių tirpiklių bei jų mišinių arba vandens, kuris vis dažniau naudojamas šiame procese. Po liejimo produktai džiovinami arba kietinami naudojant UV spinduliuotę, supjaustomi į pageidaujamas formas ir iškaitinami pašalinant visas organines medžiagas bei suteikiant mechaninį tvirtumą. Kaip keraminiai komponentai vandeninėse sistemose plačiausiai naudojami ZrO_2 , Al_2O_3 , ir AlN. Cirkonio oksidas pasižymi itin geru cheminiu, fizikiniu ir terminiu stabilumu, dideliu specifinio paviršiaus plotu bei hidrofiliškumu. Keraminės plėvelės dažniausiai naudojamos elektronikos pramonėje kaip kietųjų elektrolitų arba kietųjų oksidinių kuro elementų sudedamosios dalys. Be to, liejimo būdu gautus produktus galima pritaikyti ir daugiasluoksnių keraminių kondensatorių, laminarinių komponentų, baterijų skirtuvų, kontroliuojamos struktūros medžiagų gamyboje.

Šio magistrinio darbo tikslas buvo išnagrinėti plėvelių liejimo metodą ir suformuoti geros kokybės, gradientiškai aktytas daugiasluoksnes plėveles cirkonio oksido pagrindu, naudojant pramonį lateksinį rišiklį – uretano akrilato dispersiją vandenyje, trijų skirtingų dydžių porų formuotojus – polistireno dispersiją vandenyje, ir taikant kietinamą UV spinduliuotę. Dispersijos prieš liejimą charakterizuotos zeta potencialo ir reologiniais matavimas. Galutiniai produktai ištirti pasitelkiant skenuojančios elektroninės mikroskopijos bei Archimedo metodus.

REFERENCES

1. Bulatova R., Jabbari M., Kaiser A., Della Negra M., Andersen K. B., Gurauskis J., Bahl C. R. H., Thickness control and interface quality as functions of slurry formulation and casting speed in side-by-side tape casting, *Journal of the European Ceramic Society*, **34**, 2014, 4285 – 4295.
2. Minatto F. D., Milak P., De Noni Jr. A., Hotza D., Montedo O. R. K., Multilayered ceramic composites – a review, *Advances in Applied Ceramics*, **114**, 2015, 127 – 138.
3. Marrony M. Proton – Conducting Ceramics: From Fundamentals to Applied Research. CRC Press, 2015. 442 p. ISBN 9814613851.
4. Lv Y., Yang H. C., Liang H. Q., Wan L. S., Xu Z. K., Novel nanofiltration membrane with ultrathin zirconia film as selective layer, *Journal of Membrane Science*, **500**, 2016, 265 – 271.
5. Durif C., Fromder C., Affolter C., Lippman W., Graule T., Aquacasting – A new shaping concept for water based reactive tape casting, *Journal of the European Ceramic Society*, **35**, 2015, 3633 – 3640.
6. Albano M. P., Garrido L. B., Aqueous tape casting of yttria stabilized zirconia, *Materials Science and Engineering A*, **420**, 2006, 171 – 178.
7. Albano M. P., Genova L. A., Garrido L. B., Plucknett K., Processing of porous yttria-stabilized by tape-casting, *Ceramics International*, **34**, 2008, 1983 – 1988.
8. Duan N. Q., Tan Y., Tan D., Jia L., Chi B., Pu J., Jian L., Biomass carbon fueled tubular solid oxide fuel cells with molten antimony anode, *Applied Energy*, **165**, 2016, 983 – 989.
9. Cahn R. W., Haasen P., Kramer E. J., Brook R. J. Materials Science and Technology: a comprehensive treatment. VCH Verlagsgesellschaft mbH, Weinheim. 1996. 405 p. ISBN 3-527-26813-8.
10. Mistler R. E., Twiname E. R. Tape Casting Theory and Practice. The American Ceramic Society, 2000. 298 p. ISBN 1-57498-029-7.
11. Comparison of aqueous and non-aqueous tape casting of fully stabilized ZrO₂ suspensions, *Powder Technology*, **274**, 2015, 276 – 283.
12. Hotza D., Greil P., Review: aqueous tape casting of ceramic powders, *Materials Science and Engineering*, **202**, 1995, 206 – 217.
13. Lv Z., Zhang T., Jiang D., Zhang J., Lin., Q., Aqueous tape casting process for SiC, *Ceramics International*, **35**, 2009, 1889 – 1895.
14. Chu L. W., Prakash K. N., Tsai M. T., Lin I. N., Dispersion of nano-sized BaTiO₃ powders in nonaqueous suspension with phosphate ester and their applications for MLCC, *Journal of the European Ceramic Society*, **28**, 2008, 1205 – 1212.
15. Balakrishnan J. A., Krishnan B., Panicker R. P. N., Natarajan R., Dispersion, rheology and aqueous tape casting of alumina-zirconia composites, *Advances in Applied Ceramics*, **106**, 2007, 128 – 134.
16. Harper A. C. Handbook of ceramics, glasses, and diamonds. McGraw-Hill, 2001. 848 p. ISBN 0-07-026712-X.
17. Hannink R. H. J., Kelly P. M., Muddle B. C., Transformation Toughening in Zirconia-Containing Ceramics, *Journal of the American Ceramic Society*, **83**, 2000, 461 – 487.
18. Shockelford J., Doremus R. H. Ceramic and Glass Materials: Structure, Properties and Processing. Springer Science & Business Media, 2008. 202 p. ISBN 978-0-387-73361-6.
19. Fleckenstein C., Mochales C., Frank S., Kochbeck F., Zehbe R., Fleck C., Mueller W. D., Tetragonal and cubic zirconia multilayered ceramics: investigation of electrical parameters during automated EPD processing, *Advances in Applied Ceramics*, **113**, 2014, 35 – 41.

20. Chen L. B., Yttria-stabilized zirconia thermal barrier coatings – A review, *Surface Review and Letters*, **13**, 2006, 535 – 544
21. Brog J. P., Chanez C. L., Crochet A., From K. M., Polymorphism, what it is and how to identify it: a systematic review, *RSC Advances*, **3**, 2013, 16905 – 16931.
22. Santacruz I., Anapoorani K., Binner J., Preparation of High Content Nanozirconia Suspensions, *Journal of the American Ceramic Society*, **91**, 2008, 398 – 405.
23. Garrido L. B., Aglietti E. F., Mullite-zirconia composites: Effect of citric acid addition on slip and cast properties, *Journal of Materials Science*, **40**, 2005, 5161 – 5166.
24. Hunter R. J., *Foundations of Colloid Science*, Oxford University Press, 2004. 806 p. ISBN 0-19-850502-7..
25. Russel W. B., Saville D. A., Schowalter W. R., *Colloidal Dispersions*, Cambridge University Press, 2001. 526 p. ISBN 052142600.
26. Jingxian Z., Dongliang J., Weisensel L., Greil P., Binary solvent mixture for tape casting of TiO₂ sheets, *Journal of the European Ceramic Society*, **24**, 2004, 147 – 155.
27. Picchio M. L., Passegi Jr. M. C. G., Barandiaran M. J., Gugliotta L. M., Minori R. J., Waterborne acrylic-casein latexes as eco-friendly binders for coatings, *Progress in Organic Coatings*, **88**, 2015, 8 – 16.
28. Koh Y. H., Lee E. J., Yoon B. H., Song J. H., Kim H. E., Effect of Polystyrene Addition on Freeze Casting of Ceramic/Camphene Slurry for Ultra-High Porosity Ceramics with Aligned Pore Channels, *Journal of the American Ceramic Society*, **89**, 2006, 3646 – 3653.
29. Novais R. M., Seabra M. P., Labrincha J. A., Ceramic tiles with controlled porosity and low thermal conductivity by using pore-forming agents, *Ceramics International*, **40**, 2014, 11637 – 11648.
30. Pia G., Casnedi L., Sanna U., Porous ceramic materials by pore-forming agent method: An intermingled fractal units analysis and procedure to predict thermal conductivity, *Ceramics International*, **41**, 2015, 6350 – 6357.
31. Schmidt C. G., Hansen K. K., Andersen K. B., Fu Z., Roosen A., Kaiser A., Effect of pore formers on properties of tape cast porous sheets for electrochemical flue gas purification, *Journal of the European Ceramic Society*, **36**, 2016, 645 – 653.
32. Karaca N., Balta D. K., Ocal N., Arsu N., Thioxanthone of Fluorenone: Visible Photoinitiator for Radical Polymerization, *Journal of Polymer Science*, **54**, 2016, 1012 – 1019.
33. Bail R., Patel A., Yang H., Rogers C. M., Rose F. R. A. J., Segal J. I., Ratchev S. M., The effects of a type I photoinitiator on cure kinetics and all toxicity in projection – microstereolithography, *Procedia CIRP*, **5**, 2013, 222 – 225.
34. Sakar-Deliormani A., Celik E., Polat M., Thermal analysis and microstructural characterization of ceramic green tapes prepared by aqueous tape casting, *Journal of the Thermal Analysis and Calorimetry*, **94**, 2008, 663 – 667.
35. Akbari-Fakhrabadi A., Mangalaraja R.V., Sanhneza F. A., Avila R. E., Ananthakumar S. Chan S. H., Nanostructure Gd-CeO₂ electrolyte for solid oxide fuel cell by aqueous tape casting, *Journal of Power Sources*, **218**, 2012, 307 – 312.
36. Lu Z., Jiang D., Zhang J., Lin Q., Huang Z., ZrB₂-SiC laminated ceramic composites, *Journal of the European Ceramic Society*, **32**, 2012, 1435 – 1439.
37. Arunkumar K. V., Panicker R. N., Vasanthakumari K. G., Satheesh M., Raghu N., Unnikrishnan N. V., Dispersion and Rheological characterization of TiO₂ Tape Casting, *International Journal of Applied Ceramic Technology*, **7**, 2010, 902 – 908.

38. Szafran M., Jach K., Tomaszewska-Grzeda A., Application of enzymes and flocculants in ceramic processing of alumina, *Journal of the European Ceramic Society*, **264**, 2004, 69 – 72.
39. Wilkens-Heinecke J., de Hazan Y., Populoh S., Aneziris C. G., Graule T., Fabrication and characterisation of cellular alumina articles produced via radiation curable dispersions, *Journal of the European Ceramic Society*, **32**, 2012, 2173 – 2185.
40. Chartier T., Hinczewski C., Corbel S., UV Curable Systems for Tape Casting, *Journal of the European Ceramic Society*, **19**, 1999, 67 – 74.
41. Banerjee S., 7 – Debinding and sintering of metal injection molding (MIM) components, *Handbook of Metal Injection Molding*, 2012, 133 – 18.
42. Gorjan L., Blugan G., Graule T., Kuebler J., Effectiveness of wick-debinding inside powder bed ceramic laminates made by tape casting, *Powder Technology*, **237**, 2015, 197 – 202.
43. Rahaman M. N. Sintering of Ceramics. CRC Press, 2007. 388 p. ISBN 142000705X.
44. Idzkowska A., Wicinska P., Szafran M., Acryloyl derivative of glycerol in fabrication of zirconia ceramics by polymerization in situ, *Ceramics International*, **40**, 2014, 13289 – 13298.
45. Vozdecky P., Roosen A., Knieke C., Peukert W., Direct Tape Casting of Nanosized Al₂O₃ Slurries Derived from Autogenous Nanomilling, *Journal of the American Ceramic Society*, **93**, 2010, 1313 – 1319.
46. Yuping Z., Dongliang J., Greil P., Tape Casting of aqueous Al₂O₃ slurries, *Journal of the European Ceramic Society*, **20**, 2000, 1691 – 1697.
47. Liu S., Ye F., Liu L., Liu Q., Li J., Preparation of Aluminium Nitride Ceramics by Aqueous Tape Casting, *Materials and Manufacturing Processes*, **30**, 2015, 605 – 610.
48. Zhang Q., Cao J., Li W., Luo X., Zhuang H., Tape Casting of Aluminum Nitride Substrates, *Key Engineering Materials*, **224**, 2002, 637 – 642.
49. Pasciak G., Prociow K., Mielcarek W., Gornicka B., Mazurek B., Solid electrolytes for gas sensors and fuel cells applications, *Journal of the European Ceramic Society*, **21**, 2001, 1867 – 1870.
50. Fergus J. W., Ceramic and polymeric solid electrolytes for lithium-ion batteries, *Journal of Power Sources*, **15**, 2010, 4554 – 4569.
51. Singhal S. C., Kendall K. High Temperature Solid Oxide Fuel Cells: Fundamentals, Design and Applications. Elsevier Ltd., 2004. 405 p. ISBN 1856173879.
52. Fergus J., Hui R., Li X., Wilkinson D. P., Zhang J. Solid Oxide Fuel Cells: Materials Properties and Performance. CRC Press, 2008. 298 p. ISBN 9781420088847.